EPRI

Materials Reliability Program (MRP) EdF Thermal Fatigue Monitoring Experience on Reactor Coolant System Auxiliary Lines (MRP - 69)

LICENSED MATERIAL

Technical Report

Materials Reliability Program (MRP) EdF Thermal Fatigue Monitoring Experience on Reactor Coolant System Auxiliary Lines (MRP-69)

1003082

Final Report, April 2002

EPRI Project Managers
J. Carey
S. Rosinski

EPRI • 3412 Hillview Avenue, Palo Alto, California 94304 • PO Box 10412, Palo Alto, California 94303 • USA
800.313.3774 • 650.855.2121 • askepri@epri.com • www.epri.com

DISCLAIMER OF WARRANTIES AND LIMITATION OF LIABILITIES

ORGANIZATION(S) THAT PREPARED THIS DOCUMENT

Electricité de France

ORDERING INFORMATION

Requests for copies of this report should be directed to EPRI Orders and Conferences, 1355 Willow Way, Suite 278, Concord, CA 94520, (800) 313-3774, press 2 or internally x5379, (925) 609-9169, (925) 609-1310 (fax).

CITATIONS

This report was prepared by

Electricité de France
6, Quai Watier
78 406 Chatou, FRANCE

Principal Investigator
F. Dulcere

This report describes research sponsored by EPRI.

The report is a corporate document that should be cited in the literature in the following manner:

Materials Reliability Program (MRP) EdF Thermal Fatigue Monitoring Experience on Reactor Coolant System Auxiliary Lines (MRP-69), EPRI, Palo Alto, CA: 2002. 1003082.

REPORT SUMMARY

The Materials Reliability Project (MRP), formed in 1999, is an association of utilities focused on reactor pressure vessel, material, and related issues. The MRP Fatigue Issue Task Group is evaluating potential effects of thermal fatigue on normally stagnant piping systems attached to reactor coolant systems. This report documents results of a series of tests conducted by Electricité de France (EdF) to quantify phenomena that may cause thermal fatigue.

Background

Thermal fatigue is caused by periodic temperature variations that occur in dead-ended branch lines off the main coolant system. Temperature variations are typically due to a periodic influx of cold (or hot) water into a region of the piping. The influx may result from random turbulence effects that cause hot water from the main coolant line to periodically penetrate into the branch line or by colder water that infiltrates the branch line from a leaking valve. The section of the branch line that is subjected to alternate cooling and heating effects may eventually experience fatigue crack initiation.

Objectives

To determine the thermal-hydraulic causes of thermal fatigue in branch lines and to establish under which conditions it may occur.

Approach

EdF performed two types of experiments. In the first, various branch lines in a number of operating nuclear plants were instrumented. The project team placed thermocouples on the top, bottom, and sides of the pipes at varying distances from the connection between the branch line and the main coolant line. Plant operating parameters also were monitored. In some cases, the team recorded data for as long as two operating cycles. This instrumentation provided sufficient data to determine where in the line the thermal cycling occurred and to quantify the magnitude of the temperature fluctuations. A second type of experiment was conducted at the Blayais plant. These tests simulated a cold-water leak across an isolation valve in a branch line. Various leak rates were simulated and pipe temperatures in the branch line between the isolation valve and the main coolant line were monitored.

Results

Data analysis showed that thermal cycling was occurring in some instrumented lines. The position and amplitude of the cycling was established. This report discusses in detail a number of physical phenomena that are believed to cause the cycling. These phenomena generally involve mechanisms that cause a periodic mixing of cold and hot water at a particular axial station in the pipe.

EPRI Perspective

MRP is conducting a comprehensive program to evaluate thermal fatigue in un-isolable piping. The program includes developing a screening method that will allow utilities to determine which pipes in a plant may be affected by the phenomenon. In support of the model's development, MRP is conducting a series of fluid-hydraulic tests in bench-scale facilities. Results of the EdF testing are extremely useful to the modeling effort because they corroborate MRP tests results with results from tests in operating plants. In addition, data from the EdF testing will be used to benchmark the MRP screening model and will allow the model to be used with increased confidence.

Keywords

Fatigue
Thermal fatigue
Thermal cycling
Leakage
Reactor coolant piping
Cracking

GLOSSARY

C

cL = crossover Leg (in the primary circuit of a Nuclear Power Plant)

CL = Cold Leg (in the primary circuit of a Nuclear Power Plant)

CVC = Chemical and Volume Control system

D

D = internal diameter (thermohydraulic diameter)

DAT = Digital A Tape

Dead-end section = piping situated between the first and the second isolation valve

E

EDF = Electricité De France (French Electricity Utility)

EPRI = Electric Power Research Institute

Equipressurized situation = when dead-end section pressure is equal to primary pressure

H

HL = Hot Leg (in the primary circuit of a NPP)

HHSI = High-Head Safety Injection

L

L = Cumulative Length of piping (measured along axis)

M

MHSI = Medium-Head Safety Injection

N

Non-isolable section = piping situated between the nozzle and the first isolation valve

NP = Nuclear Power

NPP = Nuclear Power Plant

P

PCP = Primary Coolant Pump

Pressure balance = occurs in equipressurized situation

PWR = Pressurized Water Reactor (type of NPP)

PZR = Pressurizer

R

RCS = Reactor Coolant System

RIS = French acronym for Safety Injection System

RHR = Reactor Heat Removal

S

SIS = Safety Injection System

SIS accu = accumulator injection

SG = Steam Generator

SPS = Standardized plant series

V

VDS = Vent and Drain System

CONTENTS

LIST OF FIGURES

LIST OF TABLES

1
INTRODUCTION

Different fatigue-related incidents which occurred throughout the world on the auxiliary lines of the Reactor Coolant System (e.g., SIS, RHR, CVC) have led EDF to conduct a research program in order to find out the origins and the consequences of these problems.

The Research and Development Division of EDF largely contributed to this program through the implementation of in situ measurements related to thermal fatigue on some of its own nuclear power plants in order to investigate and characterize different fatigue-related incidents which had occurred worldwide on the auxiliary lines of the RCS. The data obtained from these measurements (1993 - 2000) enabled EDF to improve its knowledge of thermohydraulic phenomena causing defects on dead leg lines. It represents a significant amount of data. From 1993 up to now, the instrumentations (34 lines on the whole) were carried out with the objectives of accurately characterizing the phenomena affecting the dead legs and determining the parts of the lines affected. The sensor positions (thermocouples and pressure sensors) were selected consequently on each type of unit installed in France. The strategy of standardized plants allowed the conclusions of the study to be applied to all power plants operated in France. The data acquisition for this type of instrumentation lasted one or more cycles in order to properly characterize the phenomena. The data base obtained made it possible to better comprehend the severity of the thermohydraulic phenomena affecting the instrumented lines.

Basic information on the data provided to EPRI is described in part 2. In order to provide conclusions from the EDF experience about the generic thermohydraulic phenomena that can lead to thermal fatigue, an analysis of the data is presented in part 3, based on all relevant data available in the EDF data base. Part 4 aims at characterizing more specifically two phenomena thought to have caused defects on Class 1 piping.

2 CONTENT AND FORMAT OF EDF DATA

2.1 Introduction

The data provided by EDF concern two instrumentations performed on two different Westinghouse design 900 MW nuclear power plants (Blayais 1 and Dampierre 1). The instrumentation consisted mainly of thermocouples welded on the external surface of the piping. The primary data related to reactor operation were also recorded in order to be correlated with local data.

This chapter aims at providing all information needed for data analysis.

EDF provided data of the following auxiliary lines (for each, a description of the instrumentation is presented in Appendix A):

Blayais 1 (see A-2 to A-7)

- SIS in Hot Leg 1: Safety Injection System in Hot Leg 1 (injection tests & other data)
- SIS in Hot Leg 2: Safety Injection System in Hot Leg 2 (injection tests & other data)
- SIS in Hot Leg 3: Safety Injection System in Hot Leg 3 (injection tests & other data)
- RHR suction in Hot Leg 2 (other data)
- Drain line off crossover Leg 2 and excess letdown (other data)
- Drain line off crossover Leg 3 (other data)

Dampierre 1 (see A-8)

- SIS in Hot Leg 1: Safety Injection System in Hot Leg 1 (one cycle data)

The Appendix A graphs and tables are explained in Section 3.3.

The data of Blayais 1 and Dampierre 1 were recorded on CD ROMs provided separately to EPRI.

2.2 Format

The data were recorded on CD ROMs in an ASCII format. The date format is (dd/mm/yy hh/mm/ss). The decimal separator is a period (.). For specific sensors, temperature unit is (°C) and pressure unit is expressed in bars.

During data acquisition, the data were stored in several files. In order to keep a reasonable file size, the same structure was maintained on each CD ROM. File characteristics are described below.

Each file heading contains the sensor names. Table 2-1 provides the heading model used.

Table 2-1
Heading model used for data files

Date	Sensor Name	Sensor Name	Sensor Name	Sensor Name
dd/mm/yy hh:mm:ss	*value*	*value*	*value*	*value*
Date	RIS BC1 TC1S	RIS BC1 TC1I	RIS BC1 TC1M1	RIS BC1 TC1M2
30/10/95 11:45:06	323.2	315.4	321.6	323.1
30/10/95 11:45:07	323.2	315.4	321.6	323.1
30/10/95 11:45:08	323.2	315.4	321.6	323.1
30/10/95 11:45:09	323.2	315.4	321.6	323.1
30/10/95 11:45:10	323.2	315.4	321.6	323.1

2.3 Characteristics of a 900 MW power plant RCS

Figure 2-1 shows the positions of the main auxiliary lines of the RCS on a 900 MW power plant. It also indicates the position of the primary temperature sensors in Hot and Cold Legs (44 MT, 43 MT, ...). The surge line to the pressurizer is located approximately 2000mm upstream of the HL1 SIS branch.

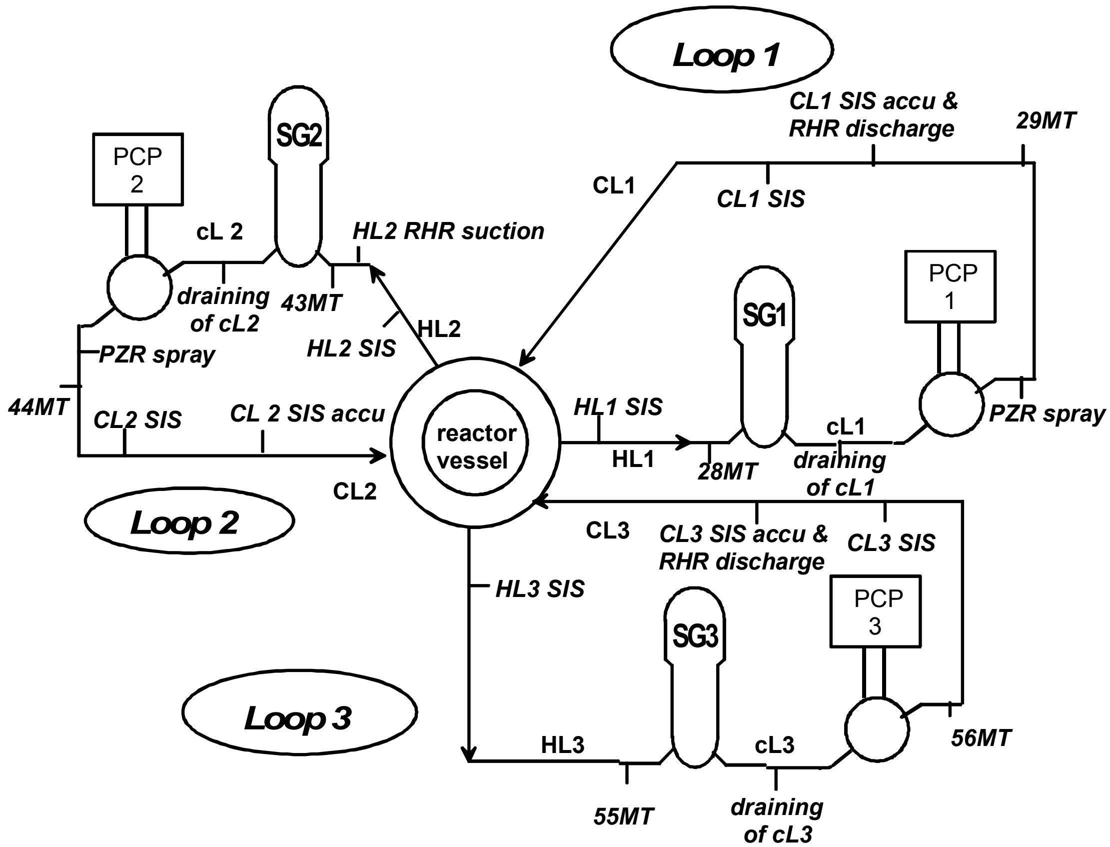

Figure 2-1
900 MW Reactor Coolant System diagram

2.4 Piping characteristics

2.4.1 Thermal insulation

Each auxiliary line is insulated from the primary nozzle to the first isolation valve. Any minor amount of air leakage that may occur around the insulation is not felt to be sufficient to alter its effectiveness.

2.4.2 Geometry

Primary piping

Hot Leg dimensions :	- external diameter	D_{ext}=865.6 mm
	- thickness	t=64.5 mm
Cold Leg dimensions :	- external diameter	D_{ext}=818.5 mm
	- thickness	t=60 mm

Auxiliary piping

Table 2-2
Auxiliary piping dimensions

	Between The Nozzle And The First Isolation Valve		After The First Isolation Valve			
auxiliary line	external diameter D_{ext} (mm)	thickness t (mm)	external diameter D_{ext} (mm)	thickness t (mm)	nozzle blend radius (mm)	distance vessel / nozzle (mm)
SIS in Hot Leg 1	168.3	18.2	168.3	18.2	18	3897.4
SIS in Hot Leg 2	168.3	18.2	168.3	18.2	18	2671.4
SIS in Hot Leg 3	168.3	18.2	168.3	18.2	18	3897.4
RHR suction in Hot Leg 2	355.6	31.8	355.6	31.8	20	2099.4
drain line off crossover leg	60.3	8.7	26.7	5.54	not available	non applicable

Except for drain lines, there is no upstream discontinuity (e.g. elbow or pump) between the reactor vessel and each dead leg nozzle. The drain line nozzle is located between the primary pump and the steam generator on the crossover leg which involves elbows. The line is located approximately 600mm downstream of the elbow.

2.4.3 Piping properties

The safety injection nozzles have no thermal sleeves. The piping material is 304L stainless steel. The ASTM classification (schedule) and the FRAMATOME class are as shown in Table 2-3.

Table 2-3
Piping characteristics

	Between the nozzle and the first valve		After the first valve	
Auxiliary line	Schedule	FRAMATOME Class	Schedule	FRAMATOME Class
SIS in Hot Leg	160	2501R	160	2501R
RHR suction in Hot Leg	140	2501R	140	2501R
drain line off crossover leg	160	2501R	160	2501R

2.5 Sensors

2.5.1 Specific sensors

The temperature sensors used are type J thermocouples welded to the external surface of the piping. The accuracy of the measurements is approximately ±3°C. However, the temperature variation uncertainty is less than 1°C.

In Appendix A, thermocouples names (partially) and positions are provided and instrumented sections indicated on isometric diagrams. The position of each section is calculated as an L/D ratio, the cumulative axis length of the auxiliary line (L) over hydraulic diameter (internal diameter D). L is the distance between the instrumented section and the primary nozzle. These dimensions used to be calculated without taking into account the connection between the primary leg and the auxiliary line. Yet, to characterize thermohydraulic phenomena, it is better to take the origin at the primary leg internal skin, which is the turbulence source. (Note: This is why the dimensions L/D are different compared to the EDF report "Synthesis of available data related to dead leg instrumentation" (HP - 17/00/045/A). The connection length was about two hydraulic diameters long.)

The name of a thermocouple is usually *l TC ip [j]*,

- *l* is the line name (for example RIS BC 2 which means SIS in HL2)
- *i* is the instrumented section number,
- *p* is the position (S for high, I for bottom, M for intermediate)
- *j* is the number that discriminates several intermediate positions, if needed,

except for the two sensors RIS HP TC 1S & RIS HP TC 1I which correspond to section 1 top and bottom pipe locations, situated upstream of the isolation valve RIS 22 VP (see Figure 2-2).

For other specific sensors, YP means pressure sensor. The pressure measurements accuracy is about ±1 bar.

2.5.2 Signals of operation

In order to be correlated with local data, reactor operation signals were recorded. Some of them (Table 2-4 & 2-12) are useful in helping to interpret the data. Therefore, they have been added to the specific sensors.

2.6 Blayais 1

Blayais 1 instrumentation was carried out from 1994 to 1996 during two cycles, which represents a significant amount of data. Therefore, injection tests data excepted, only periods showing significant transient, cycling and stable temperature loading are provided on CD ROM 1. Relevant signals of operation of the instrumentation are described in Table 2-4.

Table 2-4
Blayais 1 signals of operation

Reference	Unit	Measurement
RCP 28 MT	°C	Hot Leg 1 temperature
RCP 43 MT	°C	Hot Leg 2 temperature
RCP 55 MT	°C	Hot Leg 3 temperature
RCP 29 MT	°C	Cold Leg 1 temperature
RCP 44 MT	°C	Cold Leg 2 temperature
RCP 56 MT	°C	Cold Leg 3 temperature
RCP 25 MD	%	primary flow 1
RCP 40 MD	%	primary flow 2
RCP 52 MD	%	primary flow 3
RCP 37 MP	bar	primary pressure
RCP 04 MP	bar	RHR pressure
PUI RPN	%	nuclear power

The data are recorded on CD ROM 1 provided separately to EPRI.

- directory inj_tests: injection tests
- directory other_data: other relevant data extracted from the two cycles of monitoring

2.6.1 Injection tests

With an aim at better understanding the risks related to a leak of the isolation valves between the main primary system (155 bars) and the CVC (180 bars), in particular responsible for the incidents of Farley and Tihange, a specific instrumentation was performed on Blayais 1, a Westinghouse design 900 MW nuclear power plant. It consisted of creation of a bypass of one of the isolation valves (RIS 21 VP) equipped with one regulating valve, one isolation valve, one flow reducer (internal diameter 1.5 mm) and one flow meter in order to simulate a leakage with variable flow from CVC towards the primary system (Figure 2-2). This device allowed the simulation of stages of known flow rate from 10 to 300 l/h while measuring its consequences in terms of temperature and pressure. The flow meter Q RIS 701 MD measured the cold water flow injected from the CVC to the RCS. The flow meter unit was l/h. Two pressure sensors were used (RIS BC 05 YP and RIS BC 06 YP).

The power plant was operating at 100% nuclear power since August 27, 1995.

The different steps of the tests were precisely recorded:

- testing started on October 30th, 1995 at 9:30 a.m. (alignment of the bypass line of the RIS 21 VP)
- injection started at 9:35 a.m., 3-hour steps injections were performed from 5 l/h to 300 l/h until October 31st, 1995 at 7:30 a.m.
- injection was reduced to 108 l/h at 7:30 a.m., to 70 l/h around 10:00 a.m., and to 5 l/h around 12:30 p.m. (end of tests at 2:05 pm).

Cold-water injection lasted 28.5 hours, which corresponds to a total injected volume of 3406 liters.

The data of Blayais 1 injection tests were forwarded to EPRI in their entirety. Figure 2-2 is a functional diagram of the specific instrumentation.

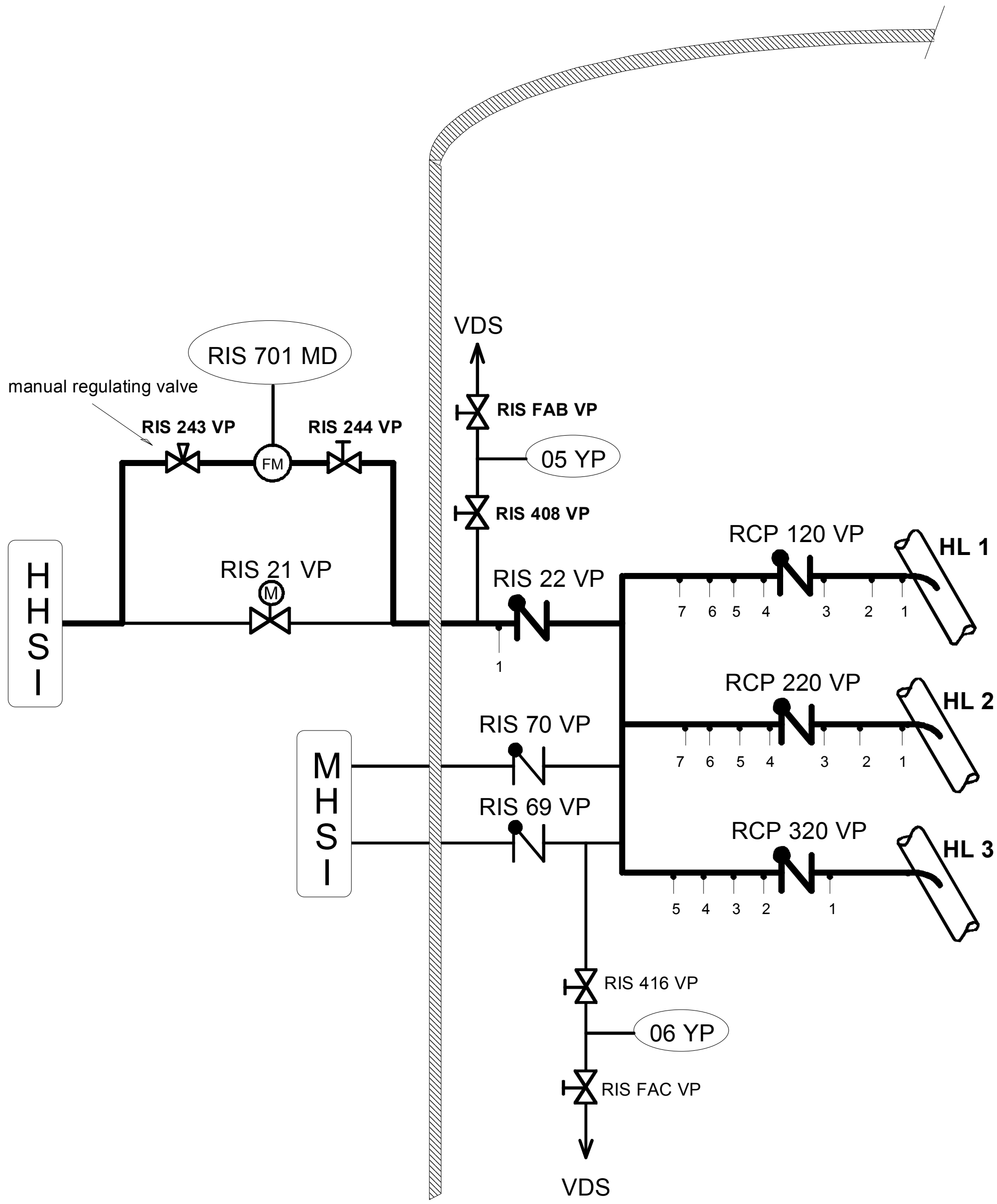

1, 2, 3 ... = instrumented section number
06 & 05 YP = pressure sensor
RIS 701 MD = flow meter
M = motorized valve

Figure 2-2
Blayais 1 injection tests diagram

Figure 2-3 and Table 2-5 give positions and elevations of the Hot Legs, the first elbow, the first isolation valve, and the second elbow for the three SIS in Hot Leg lines. Some dimensions are not real dimensions but represent the cumulative length of the auxiliary lines. All branches shown in Figure 2-3 are oriented 30-degrees upward from the horizontal. The elevation of the branch inlet is approximately 9080mm. The dimensions indicated are horizontal lengths measured to the inside surface of the pipe.

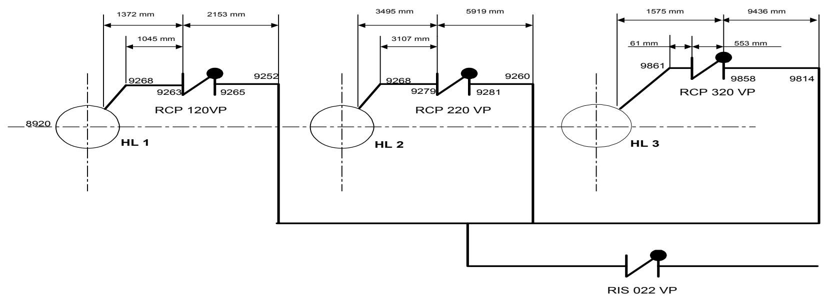

Figure 2-3
Blayais 1 SIS in Hot Leg positions and elevations

Table 2-5
Blayais 1 SIS in Hot Leg positions and elevations

	Valve Elevation	Valve/Hl Nozzle Dimension	Valve/Vertical Line Dimension	Valve Dimension	Units
HL 1	9265	1372	1600	553	mm
HL 2	9281	3495	5366	553	mm
HL 3	9858	1575	9436	553	mm

Table 2-6 presents file characteristics for the data recorded on the CD ROM.

Table 2-6
Blayais 1 injection test file characteristics

Directory	File	Start		End		Acquisition	Size	Comment
		Date	Time	Date	Time	Rate (S)	(MB)	
inj_tests	essai50	29/10/1995	19:57:02	30/10/1995	08:29:23	10	2.85	100% NP
inj_tests	essai60	30/10/1995	09:15:29	30/10/1995	10:59:07	1	3.93	10l/h injection
inj_tests	essai61	30/10/1995	11:01:54	30/10/1995	11:43:51	10	.163	stability wait
inj_tests	essai62	30/10/1995	11:45:06	30/10/1995	13:59:39	1	5.09	30 l/h injection
inj_tests	essai63	30/10/1995	14:01:19	30/10/1995	14:25:22	10	.943	stability wait
inj_tests	essai64	30/10/1995	14:26:48	30/10/1995	16:08:46	1	3.85	70 l/h injection
inj_tests	essai65	30/10/1995	16:10:17	30/10/1995	16:49:56	10	.154	stability wait
inj_tests	essai66	30/10/1995	16:51:30	30/10/1995	20:05:40	1	7.34	120 l/h injection
inj_tests	essai67	30/10/1995	20:07:27	30/10/1995	21:01:57	10	.211	stability wait
inj_tests	essai68	30/10/1995	21:04:06	30/10/1995	22:17:38	1	2.77	stop (DAT problem)
inj_tests	essai69	30/10/1995	22:30:32	30/10/1995	23:47:24	1	2.9	170 l/h injection
inj_tests	essai70	30/10/1995	23:49:08	31/10/1995	00:29:49	10	.158	stability wait
inj_tests	essai71	31/10/1995	00:30:58	31/10/1995	02:56:00	1	5.5	277 l/h injection
inj_tests	essai72	31/10/1995	02:58:06	31/10/1995	03:38:00	10	.157	stability wait
inj_tests	essai73	31/10/1995	03:39:43	31/10/1995	05:30:05	1	4.17	298 l/h injection
inj_tests	essai74	31/10/1995	05:31:29	31/10/1995	06:28:44	10	.222	stability wait
inj_tests	essai75	31/10/1995	06:30:29	31/10/1995	08:33:21	1	4.64	101 l/h injection
inj_tests	essai76	31/10/1995	08:34:46	31/10/1995	09:25:19	10	.197	stability wait
inj_tests	essai77	31/10/1995	09:26:43	31/10/1995	11:12:12	1	3.99	70 l/h injection
inj_tests	essai78	31/10/1995	11:13:35	31/10/1995	11:30:45	10	.678	stability wait
inj_tests	essai79	31/10/1995	11:31:48	31/10/1995	14:23:21	1	6.48	5 l/h injection
inj_tests	essai80	31/10/1995	14:28:23	31/10/1995	08:54:06	10	4.2	thermal stability
total data size							60.6	

Table 2-7 presents the list of injection tests specific sensors :

Table 2-7
List of injection test sensors of Blayais 1

Reference	Unit	Reference	Unit
RIS BC1 TC1S	°C	RIS BC2 TC3S	°C
RIS BC1 TC1I	°C	RIS BC2 TC3I	°C
RIS BC1TC1M1	°C	RIS BC2 TC4S	°C
RIS BC1TC1M2	°C	RIS BC2 TC4I	°C
RIS BC1 TC2S	°C	RIS BC2 TC5S	°C
RIS BC1 TC2I	°C	RIS BC2 TC5I	°C
RIS BC1 TC2M	°C	RIS BC2 TC6S	°C
RIS BC1 TC3S	°C	RIS BC2 TC6I	°C
RIS BC1 TC3I	°C	RIS BC2 TC7	°C
RIS BC1TC3M1	°C	RIS BC 5YP	bar
RIS BC1TC3M2	°C	RIS BC 6YP	bar
RIS BC1TC3M3	°C	RIS BC3 TC1S	°C
RIS BC1TC 4S	°C	RIS BC3 TC1I	°C
RIS BC1TC 4I	°C	RIS BC3 TC2S	°C
RIS BC1TC 4M	°C	RIS BC3 TC2I	°C
RIS BC1TC 5S	°C	RIS BC3 TC3S	°C
RIS BC1TC 5I	°C	RIS BC3 TC3I	°C
RIS BC1TC 5M	°C	RIS BC3 TC4S	°C
RIS BC1TC 6I	°C	RIS BC3 TC4I	°C
RIS BC1 TC 7	°C	RIS BC3 TC5S	°C
RIS BC2 TC1S	°C	RIS BC3 TC5I	°C
RIS BC2 TC1I	°C	RIS HP TC1S	°C
RIS BC2 TC2S	°C	RIS HP TC1I	°C
RIS BC2 TC2I	°C		

2.6.2 Other data

Additional data from Blayais 1 instrumentation concern the auxiliary lines described below.

Blayais 1

- SIS in Hot Leg 1 : Safety Injection System in Hot Leg 1 (see page A-2)
- SIS in Hot Leg 2 : Safety Injection System in Hot Leg 2 (see page A-3)
- SIS in Hot Leg 3 : Safety Injection System in Hot Leg 3 (see page A-4)
- RHR suction in Hot Leg 2 (see page A-5)
- Drain line off crossover Leg 2 and excess letdown (see page A-6)
- Drain line off crossover Leg 3 (see page A-7)

Table 2-8 presents additional periods that correspond to recorded data files.

Table 2-8
Other data file characteristics of Blayais 1

Directory	File	Start		End		Acquisition	Size	Comment
		Date	Time	Date	Time	Rate (S)	(MB)	
other_data	essai127	05/05/1994	00:00:29	05/05/1994	23:58:29	10	7.44	plant stop 90% - 0%
other_data	essai128	07/05/1994	23:59:57	08/05/1994	23:57:57	10	7.24	cold shutdown to hot shutdown
other_data	essai129	08/05/1994	23:59:37	09/05/1994	23:57:47	10	7.42	power increase
other_data	essai213	01/08/1994	00:03:51	02/08/1994	00:02:11	10	7.45	power increase with 100% power stable period
other_data	essai217	05/08/1994	00:05:48	06/08/1994	00:04:08	10	7.46	power variations and hot shutdown

Table 2-9 presents the list of other data specific sensors :

Table 2-9
List of other data specific sensors of Blayais 1

Reference	Unit	Reference	Unit	Reference	Unit
RIS BC1 TC1S	°C	RIS BC2 TC2S	°C	RRA ASP2TC7S	°C
RIS BC1 TC1I	°C	RIS BC2 TC2I	°C	RRA ASP2TC7I	°C
RIS BC1TC1M1	°C	RIS BC2 TC3S	°C	VID BU2 TC1	°C
RIS BC1TC1M2	°C	RIS BC2 TC3I	°C	VID BU2 TC2	°C
RIS BC1 TC2S	°C	RIS BC2 TC4S	°C	RIS BC 5YP	bar
RIS BC1 TC2I	°C	RIS BC2 TC4I	°C	RIS BC 6YP	bar
RIS BC1 TC2M	°C	RIS BC2 TC5S	°C	RRA ASP 8YP	bar
RIS BC1 TC3S	°C	RIS BC2 TC5I	°C	RIS BC3 TC1S	°C
RIS BC1 TC3I	°C	RIS BC2 TC6S	°C	RIS BC3 TC1I	°C
RIS BC1TC3M1	°C	RIS BC2 TC6I	°C	RIS BC3 TC2S	°C
RIS BC1TC3M2	°C	RIS BC2 TC7	°C	RIS BC3 TC2I	°C
RIS BC1TC3M3	°C	RRA ASP2TC1	°C	RIS BC3 TC3S	°C
RIS BC1TC 4S	°C	RRA ASP2TC2	°C	RIS BC3 TC3I	°C
RIS BC1TC 4I	°C	RRA ASP2TC3S	°C	RIS BC3 TC4S	°C
RIS BC1TC 4M	°C	RRA ASP2TC3I	°C	RIS BC3 TC4I	°C
RIS BC1TC 5S	°C	RRA ASP2TC3M	°C	RIS BC3 TC5S	°C
RIS BC1TC 5I	°C	RRA ASP2TC4S	°C	RIS BC3 TC5I	°C
RIS BC1TC 5M	°C	RRA ASP2TC4I	°C	RIS HP TC1S	°C
RIS BC1TC 6I	°C	RRA ASP2TC5S	°C	RIS HP TC1I	°C
RIS BC1 TC 7	°C	RRA ASP2TC5I	°C	VID BU3 TC1	°C
RIS BC2 TC1S	°C	RRA ASP2TC6S	°C	VID BU3 TC2	°C
RIS BC2 TC1I	°C	RRA ASP2TC6I	°C	VID BU3 TC3	°C

2.7 Dampierre 1

In order to analyze the thermal loading which led to the two Dampierre 1 incidents (SIS in hot leg 1 cracking - non isolable piping), imputed to Farley-Tihange phenomena, EDF decided to use a specific instrumentation.

The data are recorded on CD ROM 2 (directory : dampierre) provided separately to EPRI.

Dampierre 1 is also a 900 MW power plant. Therefore, the designs of Blayais 1 and Dampierre 1 units are exactly the same. The instrumentation was based on Blayais 1 results. The monitoring concerned the safety injection line in Hot Leg 1 (see page A-8).

Figure 2-4 presents the position of pressure sensors :

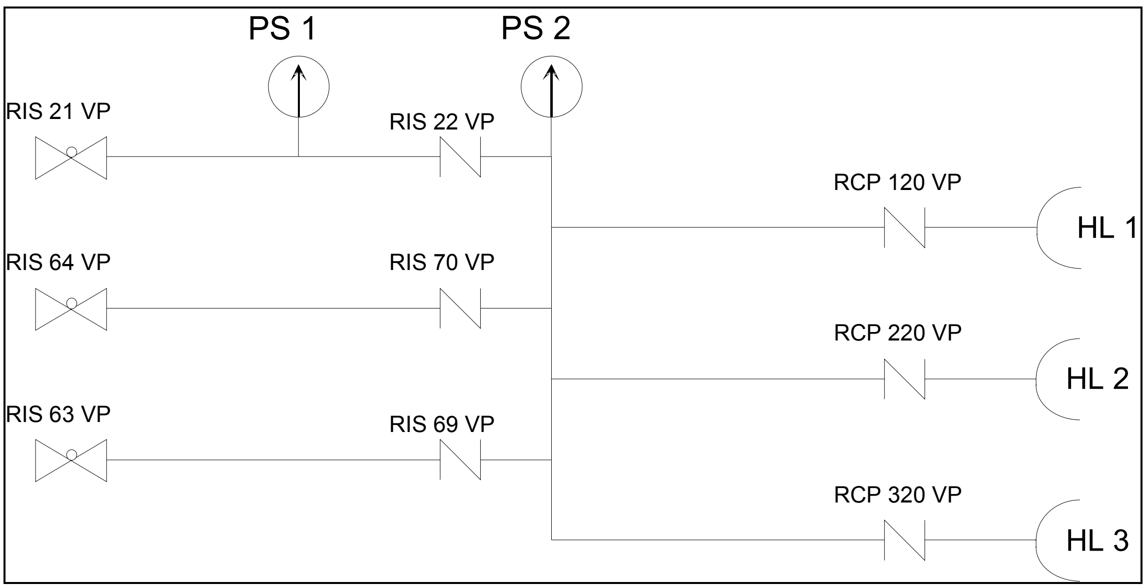

Figure 2-4
Dampierre 1 pressure sensors positions

The data was monitored from March 1998 to October 1998. The data were recorded according to the scheme shown in Table 2-10.

Table 2-10
Dampierre 1 files characteristics

Directory	File	Start		End		Acquisition	Size
		Date	Time	Date	Time	Rate (S)	(MB)
dampierre	essai1	12/03/1998	17:04:26	13/03/1998	12:18:16	1	17.5
dampierre	essai2_1	13/03/1998	12:19:57	14/03/1998	00:00:00	1	10.5
dampierre	essai2_2	14/03/1998	00:00:00	14/03/1998	12:00:00	1	10.9
dampierre	essai2_21	14/03/1998	12:00:00	15/03/1998	00:00:00	1	10.9
dampierre	essai2_3	15/03/1998	00:00:00	15/03/1998	12:00:00	1	10.9
dampierre	essai2_31	15/03/1998	12:00:00	16/03/1998	00:00:00	1	10.9
dampierre	essai2_4	16/03/1998	00:00:00	16/03/1998	12:00:00	1	10.9
dampierre	essai2_41	16/03/1998	12:00:00	17/03/1998	00:00:00	1	10.9
dampierre	essai2_5	17/03/1998	00:00:00	17/03/1998	12:00:00	1	11.0
dampierre	essai2_51	17/03/1998	12:00:00	18/03/1998	00:00:00	1	10.9
dampierre	essai2_6	18/03/1998	00:00:00	18/03/1998	10:31:08	1	9.6
dampierre	essai3	18/03/1998	10:34:36	18/03/1998	10:34:38	1	0.001
dampierre	essai12_1	18/03/1998	11:31:32	19/03/1998	00:00:00	1	11.4
dampierre	essai12_2	19/03/1998	00:00:00	19/03/1998	12:00:00	1	11.0
dampierre	essai12_3	19/03/1998	12:00:00	20/03/1998	00:00:00	1	11.0
dampierre	essai12_4	20/03/1998	00:00:00	20/03/1998	12:00:00	1	11.0
dampierre	essai12_5	20/03/1998	12:00:00	21/03/1998	00:00:00	1	11.0
dampierre	essai12_6	21/03/1998	00:00:00	21/03/1998	12:00:00	1	11.0
dampierre	essai12_7	21/03/1998	12:00:00	22/03/1998	00:00:00	1	11.0
dampierre	essai12_8	22/03/1998	00:00:00	22/03/1998	12:00:00	1	11.0
dampierre	essai12_9	22/03/1998	12:00:00	23/03/1998	00:00:00	1	11.0
dampierre	essai13	23/03/1998	08:50:35	30/03/1998	00:00:05	10	14.6
dampierre	essai15	30/03/1998	01:01:59	06/04/1998	01:01:49	10	15.4
dampierre	essai16	06/04/1998	01:03:39	13/04/1998	01:03:29	10	15.4
dampierre	essai17	13/04/1998	01:04:41	20/04/1998	01:04:31	10	15.4
dampierre	essai18	20/04/1998	01:06:23	27/04/1998	01:06:23	10	15.4
dampierre	essai19	27/04/1998	01:08:16	04/05/1998	01:08:06	10	15.4
dampierre	essai20	04/05/1998	01:09:57	11/05/1998	01:09:57	10	15.4
dampierre	essai21	11/05/1998	01:11:50	18/05/1998	01:11:50	10	15.4
dampierre	essai22	18/05/1998	01:13:42	18/05/1998	11:45:32	10	1
dampierre	essai23	18/05/1998	12:40:07	25/05/1998	00:00:07	10	14.2
dampierre	essai25	25/05/1998	00:02:00	01/06/1998	00:02:00	10	15.4
dampierre	essai26	01/06/1998	00:03:52	08/06/1998	00:03:42	10	15.4

Table 2-10 (continued)
Dampierre 1 files characteristics

dampierre	essai27	08/06/1998	00:04:55	15/06/1998	00:04:55	10	15.4
dampierre	essai28	15/06/1998	00:06:48	22/06/1998	00:06:38	10	15.4
dampierre	essai29	22/06/1998	00:08:13	24/06/1998	10:20:13	10	5.3
dampierre	essai30	24/06/1998	11:56:25	24/06/1998	12:01:15	10	0.008
dampierre	essai34	29/06/1998	00:01:28	06/07/1998	00:01:18	10	15.4
dampierre	essai35	06/07/1998	00:02:03	13/07/1998	00:01:53	10	15.4
dampierre	essai36	13/07/1998	00:03:15	20/07/1998	00:03:05	10	15.4
dampierre	essai37	20/07/1998	00:04:28	27/07/1998	00:04:18	10	15.4
dampierre	essai38	27/07/1998	00:05:40	03/08/1998	00:05:30	10	15.4
dampierre	essai39	03/08/1998	00:06:53	10/08/1998	00:06:53	10	15.4
dampierre	essai40	10/08/1998	00:08:21	17/08/1998	00:08:11	10	15.4
dampierre	essai41	17/08/1998	00:09:42	24/08/1998	00:09:32	10	15.4
dampierre	essai42	24/08/1998	00:11:03	31/08/1998	00:10:53	10	15.4
dampierre	essai43	31/08/1998	00:12:25	07/09/1998	00:12:25	10	15.4
dampierre	essai44	07/09/1998	00:13:56	14/09/1998	00:13:56	10	15.4
dampierre	essai45	30/10/1998	09:51:20	02/11/1998	00:00:00	10	15.4
dampierre	essai47	02/11/1998	00:01:31	06/11/1998	13:53:06	10	9.6
dampierre	essai48	06/11/1998	13:54:31	13/11/1998	13:54:31	10	14.7
dampierre	essai49	13/11/1998	13:55:25	16/11/1998	14:13:35	10	6.6
dampierre	essai50	18/11/1998	16:45:10	25/11/1998	16:45:00	10	15.4

Table 2-11 presents the list of specific sensors :

Table 2-11
Llist of specific sensors of Dampierre 1

Reference	Unit
YFT TC 1I	°C
YFT TC 2I	°C
YFT TC 3I	°C
YFT TC 4I	°C
YFT TC 5I	°C
YFT TC 6I	°C
YFT TC 7I	°C
YFT TC 7S	°C
YFT TC 8I	°C
YFT TC 8S	°C
YFT TC 9I	°C
YFT TC 9S	°C
YFT MP 01 (PS1)	bar
YFT MP 02 (PS2)	bar

Signals of operation of Dampierre 1 instrumentation are described in Table 2-12 :

Table 2-12
Dampierre 1 signals of operation

Reference	Unit	Measurement
RCP 25 MD	%	Primary flow 1
RCP 40 MD	%	Primary flow 2
RCP 50 MD	%	Primary flow 3
RPN	%	Nuclear power
RCP 32 MT	°C	Hot Leg 1 temperature
RCP 47 MT	°C	Hot Leg 2 temperature
RCP 59 MT	°C	Hot Leg 3 temperature
RCP 37 MP	bar	primary pressure

3 GENERIC PHENOMENA OF LOCAL THERMOHYDRAULICS

3.1 Introduction

Instrumentation of the non discharging auxiliary lines of the RCS (called dead legs) has enabled EDF to highlight some generic phenomena with low dependence upon the operation parameters. In this section, we deliberately limit the discussion to the thermohydraulic phenomena observed in dead legs under normal operating conditions of the unit. The phenomena dealt with here are vortex penetration, natural convection loops, thermal stratification, two-phase water-steam state and independent thermal cycling. In the following, we provide a detailed description of these phenomena. The entire set of results from the summary of each instrumentation campaign then allows the data related to thermal loads at 100% NP for each instrumented line to be collected and quantitative conclusions on the phenomena to be drawn.

3.2 Description

3.2.1 Vortex

This phenomenon, also called turbulent penetration, causes dead legs to heat up. The heat transfer mechanism caused by vortex is called forced turbulent convection. Several configurations can produce different consequences on its behaviour. The following presentation is limited to the general case (a horizontal auxiliary piping), where the vortex is not stopped by a valve and in which there is no cold in-leakage. The other configurations will be considered later in this document. Some of the discussion in this section is based on the results of additional mockup testing performed by EDF.

The intersection between the main piping and the auxiliary line is called the nozzle. This is the place where the turbulent flow (with a high Reynolds number) of the primary fluid undergoes shearing, thereby causing the fluid to be recycled in the dead leg. Under certain circumstances, this recycling may degenerate into a whirl. Its complex structure is made up of three zones (Figure 3-1).

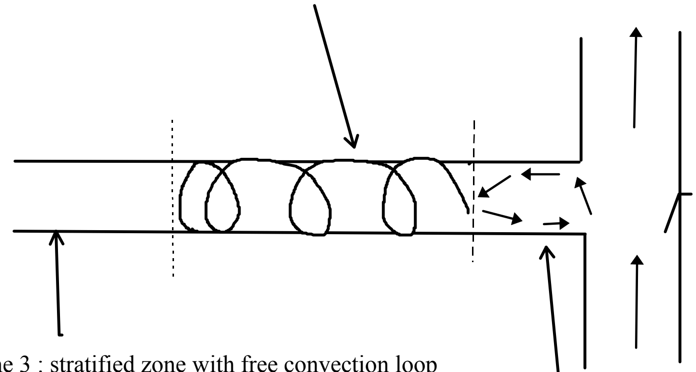

Figure 3-1
Diagram showing dead leg penetration

The flow is very disorderly in the zone next to the nozzle (the first three diameters of the dead leg). We have here a penetration vortex the axis of which is perpendicular to the nozzle plane. The vortex then becomes gradually dissymmetric and turns into a helical whirl structure. At this stage, it is made up of two interweaved helical zones, the fluid originating from the nozzle being located in the most outlying zone (Figure 3-2). The fluid returns back toward the nozzle down the center of the pipe. This phenomenon does not appear to depend on the orientation of the pipe and has been confirmed by velocity measurements made in a mock-up facility.

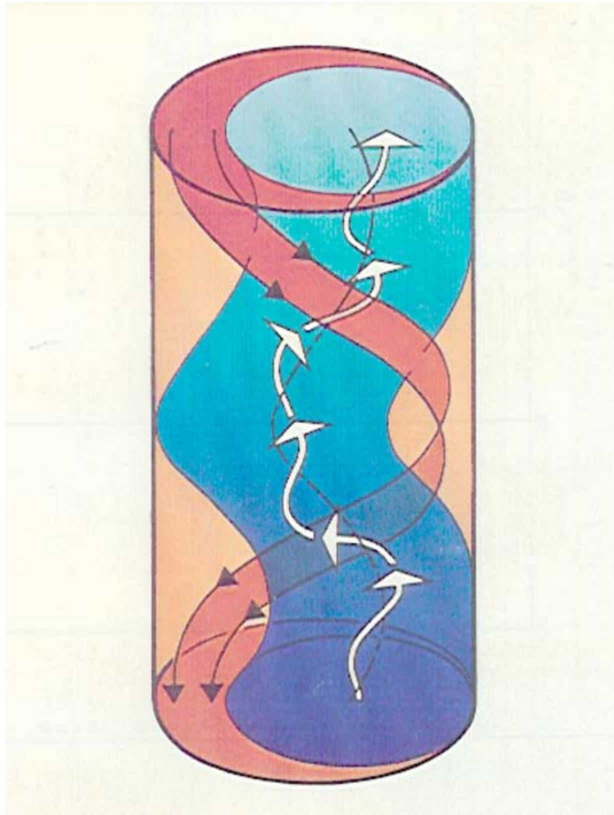

Figure 3-2
Diagram of the flow measured on mock-up

The interface between zone 2 and 3 is the seat of thermal fluctuations which are at a maximum along the bottom of the pipe and result from the interaction between the whirl and the stratified zone. The free convection loop which creates the stratification gradient is intermittently slowed down by these fluctuations which therefore can propagate throughout the stratified zone.

One of the main characteristics of the vortex is its unsteady nature that shows itself in frequent changes of direction and/or intensity. Both the direction of the swirl and the penetration depth change with time. It is difficult to assess the degree of influence of the different parameters involved on this behavior.

From a purely hydraulic standpoint, one may however state that the formation of the whirl and its intensity depend in a complex manner mainly upon the following conditions (quoted in order of ascending priority):

- the Reynolds number;
- the shape of the nozzle blend radius which strongly influences the penetration depth and possibly, to a lesser extent, the branch line/RCS diameter ratio (Figure 3-3);
- the upstream conditions (i.e., mean velocity field), on which the penetration depth is dependent.

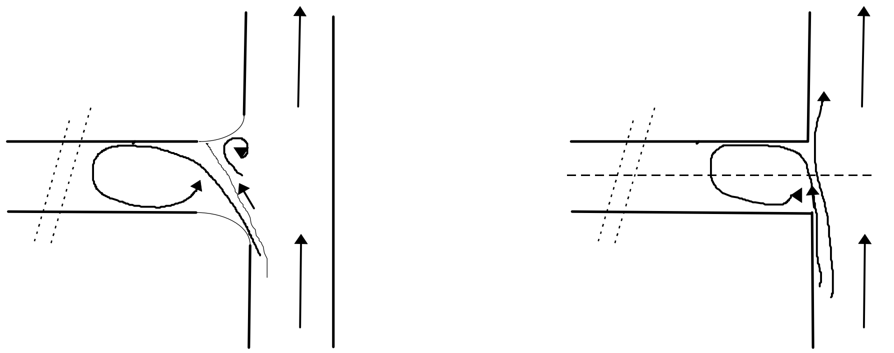

Figure 3-3
Influence of the welding chamfer on the penetration depth

The couplings between the thermal and hydraulic phenomena further add to these factors. The phenomena of conduction (fluid and solid thermal transfer) and free convection (fluid thermal transfer) are no longer negligible with respect to the forced convection in the vortex front zone (i.e., the transition region between zones 2 and 3) where the velocities become very low. These couplings probably contribute to the instability of the whirl and may have an influence on the vortex length. Indeed, a natural convection loop is likely to stop the whirl quickly.

It seems that the flow is sensitive to the slightest variations of the boundary conditions. Indeed, the thermal conditioning of two rigorously identical dead legs sometimes varies from one loop to another (of the same unit or not).

Finally, it should be stated that this phenomenon is not intrinsically harmful. It homogenizes the fluid temperature all over its length, so that the fluid temperature becomes close to that of the primary fluid.

3.2.2 Free convection loop and stratification

Natural convection (or free convection) is a heat transfer mechanism where the fluid is set in motion. The occurrence of this mechanism requires the following conditions to be met:

- a hot source;
- a cold source (with no fluid dynamic phenomena such as in-leakage from a valve);
- a line configuration in which the gravity forces permit the propagation of the heat flow;
- the fluid being in the liquid phase only, as a two-phase water-steam state acts as a brake upon free convection.

Natural convection can develop in vertical upward or horizontal piping only. A downward vertical section prevents heat propagation by free convection. Transfer then mainly takes place by conduction. In this case, the axial heat distribution decreases very quickly.

In a dead leg, when the vortex front is located in a horizontal or slightly inclined pipe section, it becomes the hot source necessary for the formation of a free convection loop within the non isolable pipe section. The fluid next to the vortex front flows upward due to mixing with the hot vortex flow. Cold fluid (which is heavier) streams to the location previously occupied by the hot water, heats up through its contact with the hot source and the cycle starts again. In the absence of a vertical pipe section (which can break the free convection loop), the latter will reach the first section valve which is then at a temperature close to that of the primary fluid.

In this case or when the vortex reaches the first valve, provided that the line configuration permits this, the valve becomes the hot source of a natural convection loop developing within the dead end line portion of the isolable piping, with a mechanism identical to that of the non isolable line section.

This mechanism is shown in Figure 3-4:

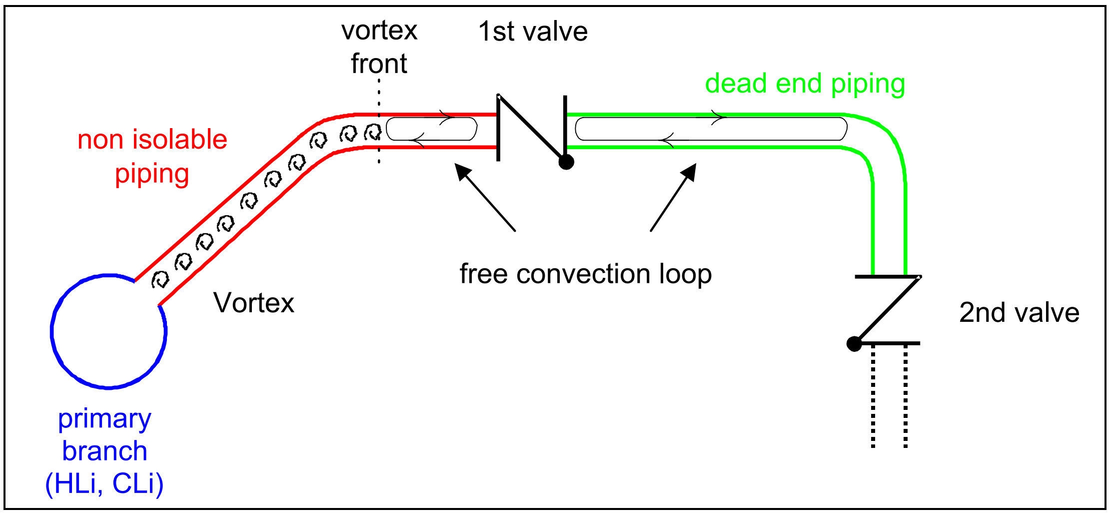

Figure 3-4
Diagram of convection loops in a dead leg

Natural convection leads to the formation of a thermal stratification gradient between the top and bottom of the pipe. Such temperature gradients create mechanical stresses in the pipe, which depend both on the amplitude and the profile of the thermal stratification. These stresses lead to overall bending of the pipe. Should the bending be excessive, it may damage the line supports.

The thermal stratification phenomenon generally occurs in systems where fluids with different temperatures may come in contact. This results in a competition between the inertia effects (depending on the velocity of the fluid) and the density effects, related to the fluid temperature. The thermohydraulic parameter that governs the formation of stratification is the Froude number (which expresses the ratio of speed effects to gravity effects). This stratification phenomenon shows itself by the presence of a hot layer in the upper part of the pipe, a cold layer in the lower part and an intermediate zone in-between. The position and thickness of this interface between cold and hot fluid develop depending on the line's temperature, pressure and flow conditions.

In dead legs, the fluid stagnates. When the formation of natural convection loops takes place, thermal stratification gradients appear between the top and bottom of the pipe. Due to the absence of circulation, physico-chemical phenomena increase the fatigue caused by the stratification. In addition to vortex instability, this phenomenon may also contribute to the deterioration of the piping (§ 4.2).

Stratification also occurs in the steam generator feed lines when flow rates are low, in particular during hot shutdowns. This case, which is not discussed in this paper, was the subject of specific instrumentations.

3.2.3 Independent thermal cycling

By "independent thermal cycling" is meant variations in temperature within a limited range and non-correlated with unit operation. Two types of thermal cycling are distinguished depending on their location: 1) thermal cycling within the non-isolable section, and; 2) thermal cycling in the dead end section. These are discussed in more detail below.

3.2.3.1 Thermal Cycling Within the Non-isolable Section

The type of cycling generally appears in the transitional area between the zone still affected by the whirl penetration and the associated convection loop (Figure 3-5). The less the vortex energy, the more important the cycling. Sometimes, lesser fluctuations can be observed in the vortex area.

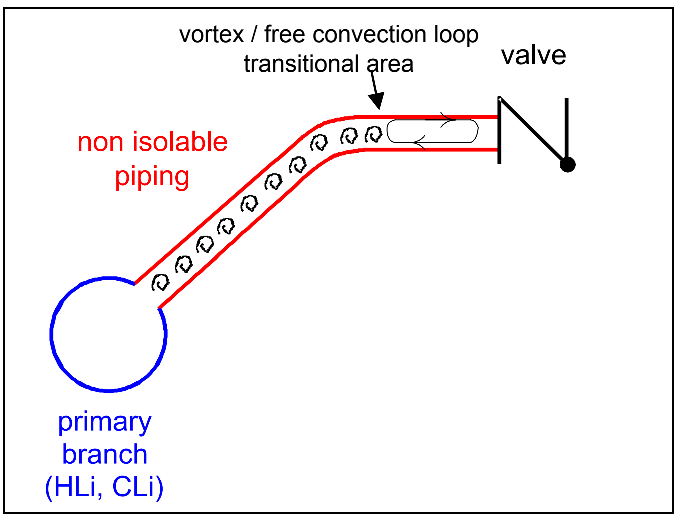

Figure 3-5
Location of cycling in the non-isolable section

In case the whirl reaches the first valve, the line temperature is very close to that of the primary line. When dealing with a horizontal section between two isolation valves, a slight difference in temperature between the top and bottom of the pipe (Figure 3-6) is often to be seen in the vicinity of the valve located on the primary side, even though one would rather expect the temperature to become homogenized by the vortex. This is due to the fact that the heat transferred through the valve leads to the formation of a natural convection loop on the opposite side of the valve. This loop tends to cool down the lower part of the valve. From this results a stratification gradient of a few degrees centigrade between the top and the bottom of the pipe in the non-isolable section.

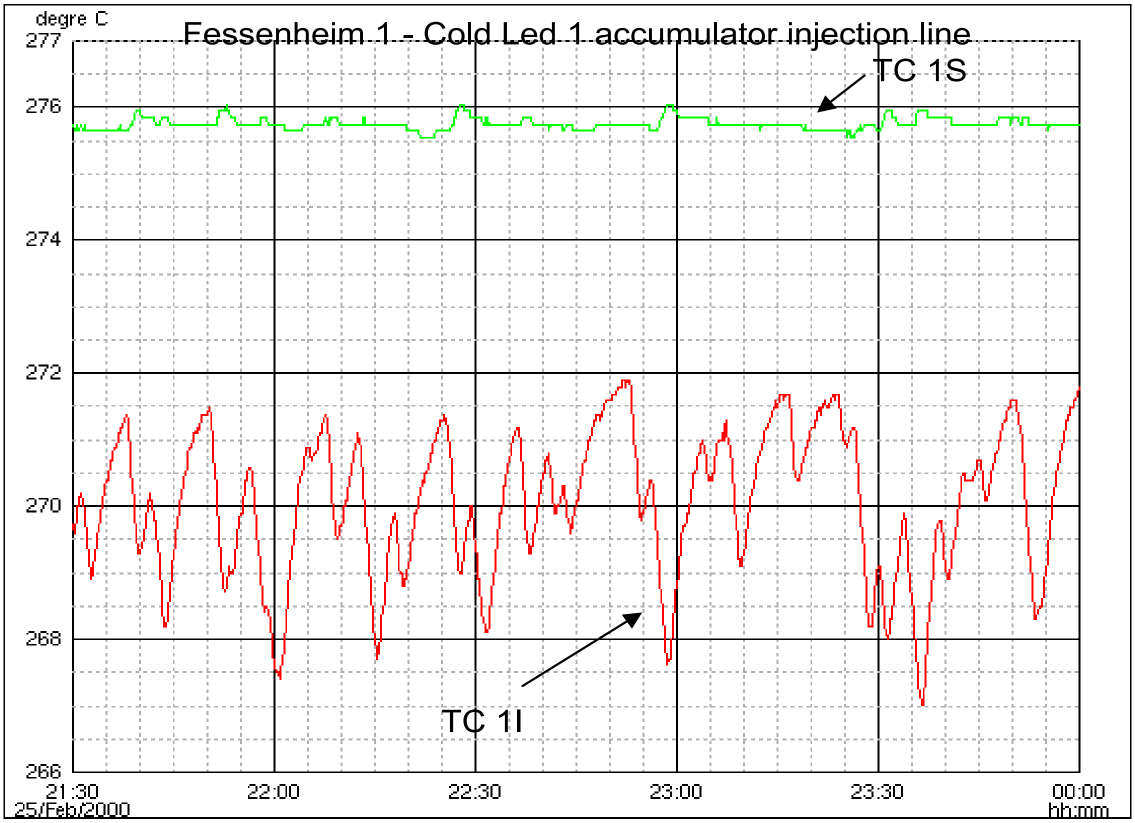

Figure 3-6
Difference in temperature on the non-isolable section

The range of thermal cycling may depend on the pressure existing in the dead-end section. Downstream of the check valve RCP 120 VP, for the Blayais 1 Hot Leg 1 injection line, it rises from approximately 9°C in a non-pressurized common header situation (5 bar) to 21°C in pressurized condition (155 bar). In addition to the thermal conduction taking place through the check valve, it is possible that the leakage of the latter, favored by the balance of pressure, keeps up a cold layer the interaction of which with the vortex leads to thermal fluctuations.

On some longer downward vertical lines (such as the Blayais 1 Cold Leg 3 accumulator injection line), the cycling is noticed along the upper pipe surface (Figure 3-7). It is combined with substantial thermal stratification (ΔT_{2S-2I} = 85°C in this case). This can be explained by the fact that the vortex front is located in the zone of the vertical elbow (located at a distance of about 18 D from the nozzle) and that a hot stream, the temperature of which varies depending on the instability of the whirl, heats up the upper surface of the pipe, thus creating a strongly stratified zone. These variations remain within a limited range (<28°C), compared with the thermal shocks which are the subject of 4.2.

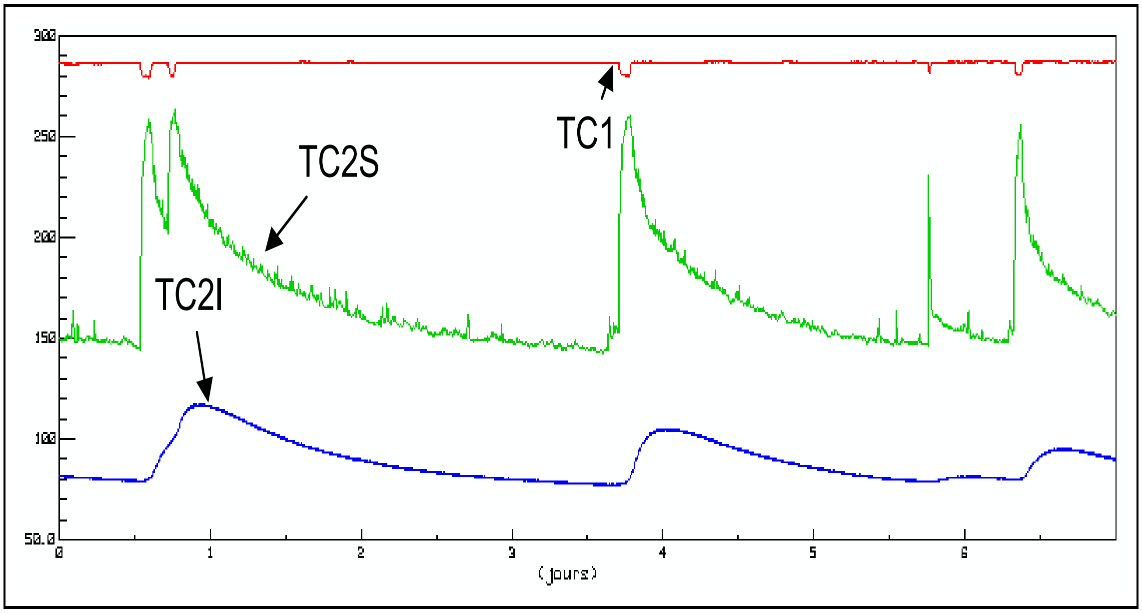

Figure 3-7
Stratification, cycling and thermal shocks in the line RIS AQ BF3 of Blayais 1

3.2.3.2 Thermal Cycling in the Dead-end Section

The cycling taking place in this section is either due to variations in the primary pressure in the equipressurized situation (Figure 3-8) or to fluctuations in the position of the interface water / saturated mixture of water and steam. In the first case, it concerns small displacements of fluid caused by variations in the primary pressure which show themselves by cycling (i.e., a small reduction in pressure allows a small flow of cold water past the check valve which cools the fluid near the thermocouple).

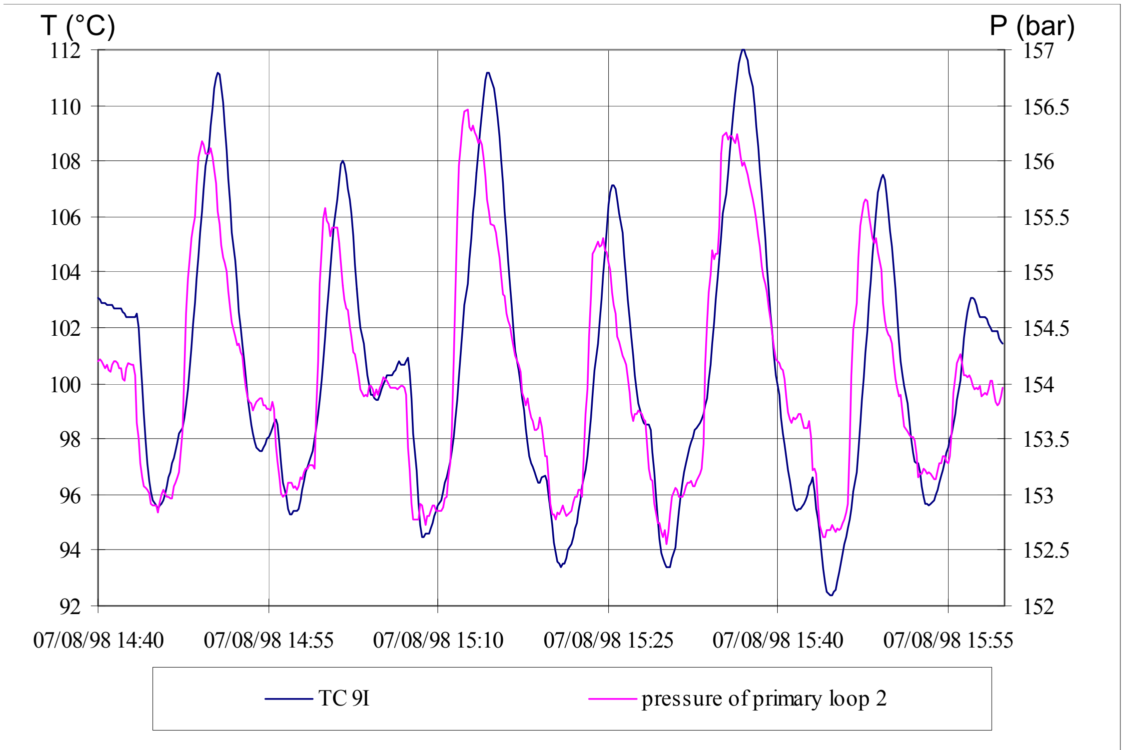

Figure 3-8
Thermal cycling due to variations in the primary pressure (Dampierre 1 Hot Leg 1 SIS)

3.3 A thermal load report for each line

Table 3-1 shows relevant data from instrumentation on several units.

Table 3-1
List of instrumented units

Unit	Abbreviation	Standardized Plant Series	Power (MW)
Blayais 1	BLA1	CPY	900
Cruas 4	CRU4	CPY	900
Chinon B3	CNB3	CPY	900
Dampierre 1	DAM1	CPY	900
Golfech 2	GOL2	P'4	1300
Fessenheim 1	FES1	CP0	900

Table 3-2 gives the list of instrumented auxiliary lines, results of which are used here, and the Appendix A page number where some lines are described.

Table 3-2
List of instrumented lines

Unit	Auxiliary Line	Abbreviation	Page
Blayais 1	Hot Leg 1,2,3 injection line	HL1,2,3 SIS	A-2,3,4
	Cold Leg 1,2,3 injection line	CL1,2,3 SIS	
	Cold Leg 1,3 accumulator injection line & RHR discharge	CL1,3 SIS accu	
	Cold Leg 2 accumulator injection line	CL2 SIS accu	
	Hot Leg 2 RHR suction	HL2 RHR suction	A-5
	Drain line off crossover Leg 2 & excess letdown	cL2 drain	A-6
	Drain line off crossover Leg 3	cL3 drain	A-7
Cruas 4	Cold Leg 1,2,3 injection line	CL1,2,3 SIS	
Chinon B3	Hot Leg 1,2,3 injection line	HL1,2,3 SIS	
Dampierre 1	Hot Leg 1 injection line	HL1 SIS	A-8
Golfech 2	Hot Leg 4 RHR suction	HL4 RHR suc	
	Cold Leg 1 RHR discharge	CL1 RHR dis	
	Hot Leg 2 injection line	HL2 SIS	
	Cold Leg 4 injection line	CL4 SIS	
	Drain line off crossover Leg 1,2	cL1,2 drain	
	Drain line off crossover Leg 3 & excess letdown	cL3 drain	
	Drain line off crossover Leg 4 & CVC letdown	cL4 drain	
Fessenheim 1	Cold Leg 1,3 accumulator injection line & RHR discharge	CL1,3 SIS accu	
	Cold Leg 2 accumulator injection line	CL2 SIS accu	

We use here, for each instrumented line, the balance of the average thermal loads at 100% NP and stabilized temperatures, i.e. when temperature variations around their average value remain low in time. This balance is representative for the operation of the unit. The objective of this section is to collect these results and to characterize in a simple manner the generic phenomena involved. For select data identified above, the information related to the average loads is gathered in Appendix A on one page per line, each page containing a table, an isometric diagram and a graph. The same method applied for all lines of Table 3-2 and allowed conclusions to be drawn in Section 3.4. The content of the Appendix A tables are as shown in Table 3-3.

Table 3-3
Information content of tables in Appendix A

Information	Comment
series	CP0, CPY, P'4 and N4
line	unit and branch pipe description
section	section mark (Si)
L/D	position of the section [(1)]
pressure	Bar
thermocouples	item number and position of the thermocouples per section - temperature in °C
isolating valve	diagram and item number
orientation	spatial orientation indicated by a letter [(2)]
heat insulation	shaded
vortex length	represented by a stroke [(3)]
length of natural convection loop	represented by a stroke [(3)]
stratification range	temperature gradient between top and bottom of pipe in °C
two phase state	indicated by a cross [(4)]
thermal cycling	indicated by a cross [(5)]
geometrical data	in " (inch) [(6)]
primary temperature	°C
primary flow rate	m^3/h

[(1)] To make it possible to compare the thermohydraulic phenomena between different lines, the length of piping is indicated in hydraulic diameters (internal diameter of the piping). The origin is the intersecting point of the inner wall of the primary coolant loop with the axis of the auxiliary line. Possible differences in the section positions with respect to previous documents are due to the choice of this origin.

(2) The meaning of the different letters used is explained in Table 3-4.

Table 3-4
Meaning of the letters used for indicating the section orientation

Letter	Meaning
H	horizontal
V	vertical
I	inclined
D	downward (from RCS to auxiliary line)
U	upward (from RCS to auxiliary line)
E	elbow

Example: ID means "inclined downward section".

(3) To determine whether the whirl and natural convection loop are present, one has to interpret the temperature values, the presence of cycling, stratification and the geometry and orientation of the line. As both phenomena are often combined, an overall analysis of the phenomena is necessary. The tables tell us if such phenomenon is present in a given section. Therefore the strokes do not represent the actual length of the phenomena, but provide the reader with a good view of the phenomena. Their interpretation is sometimes tricky, in particular when the vortex does not reach the section valve and also when one cannot easily distinguish the whirl and the convection loop, if the latter exists. The different cases to be interpreted are described in the following:

- The vortex front is located in a downward vertical section. The thermohydraulic conditions are unstable and heat transfers take place through conduction. The decrease in temperature is exponential. This case only concerns the Blayais 1 Cold Leg 3 injection line and can be interpreted straightforwardly.

- The vortex front is located in a horizontal or slightly inclined section; the thermohydraulic conditions are unstable. Natural convection takes place and the effect of this is a temperature gradient.

- The vortex front is located in a vertical upward section. The situation is stable. Even though heat transfer also takes place through free convection, the transition zone cannot be assessed by external temperature values. In this type of configuration, the whirl length probably exceeds that of the other configurations (this is due to the combination of the thermal and hydraulic effects). For the few sections in which this zone is vague, it is considered that one is in presence of a whirl (slight over-estimation of the whirl length).

(4) A cross indicates that, depending on the pressure in the dead-end section, the zone may show a two-phase state. The water saturation curve is shown in Figure 3-9.

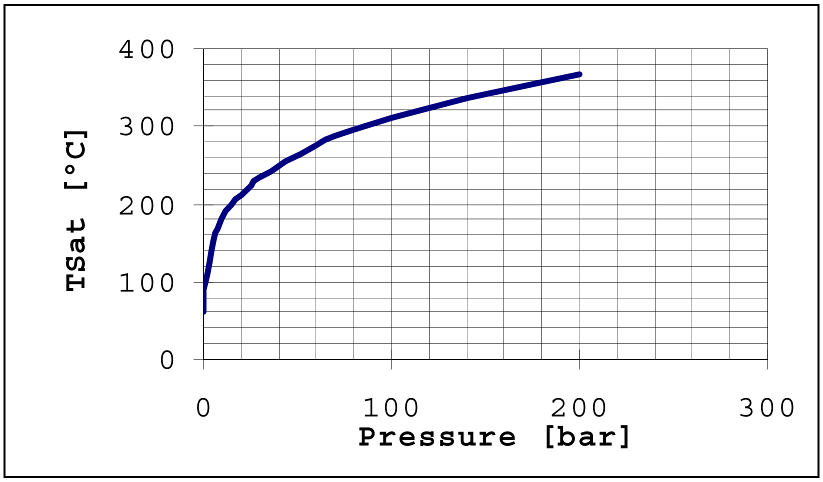

Figure 3-9
Water saturation curve

(5) The presence of thermal cycling with a range exceeding 5°C is indicated. UG or LG correspond to variations taking place along the upper or lower pipe surfaces.

(6) The correspondence between the geometric data in inches and mm (internal diameter and wall thickness) is provided in Table 3-5.

Table 3-5
Correspondence between the geometric data in inches and mm

Diameter (Inches)	Internal Diameter (mm)	Thickness (mm)	Schedule
14	292	31.8	140
12	257.3	33.3	160
12	266.7	28.6	140
10	215.8	28.6	160
10	222.2	25.4	140
8	173.1	23	160
6	131.9	18.2	160
2	42.9	8.7	160
¾	15.6	5.54	160

Each auxiliary line is represented by a 3D isometric diagram positioned within a rectangular parallelepiped, to provide for easy understanding of the spatial orientation of the different sections. The position of the instrumented sections is shown by an arrow.

To ensure improved viewing of the thermal loads and stratification gradients, the curves corresponding to the temperatures along the upper and lower pipe surfaces according to the L/D ratios are traced on a graph when the line is sufficiently instrumented and complete the line report.

Remark:

The different colors of the values provided by the different temperature sensors either correspond to periods in which the thermal loads varied or to periods in which the pressure in the dead-end section is different.

There is no functional difference between these periods. The thermal conditioning of a line can vary naturally without any correlation with the unit operation. Very often, it is the random character of the whirl which is responsible for these variations. The pressure in the dead-end section may also vary during a cycle, in particular during the loss of pressure balance, a case that may result from valve leakage. As the temperature of the fluid is related to its pressure, the differences in thermal loads may correspond to variations in pressure.

3.4 Review of on site instrumentation

The purpose of this section is to draw the quantitative conclusions on the basis of average thermal loads with respect to the previously-described generic phenomena.

The whirl penetration in the auxiliary line, as well as the free convection, exist almost systematically in dead legs. A number of lines are also the seat of autonomous thermal cycling.

Appendix B presents a summary of phenomena that may be observed in most dead legs. For each line, as a function of the characteristic length (L/D), we indicate the zones where the instrumentation has revealed vortex and convection loop phenomena. In this Appendix, mention is also made of the zones where the presence of a two-phase state was detected.

It should be noted that the drain lines off the crossover Legs were poorly instrumented compared to the other lines. For Golfech 2, these lines have been left out of Appendix B because it is impossible to quantify the phenomena length.

The sensors were positioned in such a way that they were capable of capturing the various phenomena involved. The sensors thus enabled us to affirm that we were or that we were not in the presence of the phenomenon considered. Between two instrumented sections, there is often an area of uncertainty. Table 3-6 shows the legend of the summary table in Appendix B:

Table 3-6
Legend of Appendix B

	: vortex
	: convection loop
	: diphasic water-steam state and convection loop
	: isolation valve
	: uncertainty area of vortex
> <	: uncertainty area of diphasic state end
> <	: uncertainty area of convection loop end

3.4.1 Vortex

The results provided in Appendix B confirm that the vortex phenomenon can be observed in all dead legs of French nuclear power plants.

Despite its dispersion, the results allow one to draw quantitative conclusions. In all the cases where the vortex does not reach the first isolation valve (except for the Chinon B3 Hot Leg 2 injection line, where the instrumentation does not allow us to prove that the phenomenon exists), we have whirl length bounds as shown in Table 3-7. (Note: For vertical pipes followed by horizontal runs, if cycling is observed along the upper surface of the elbow, it is assumed that the vortex front is located at the elbow and that the minimum and maximum values are the same.)

Table 3-7
Vortex length bounds

Line	L/D_{min}	L/D_{max}
BLA1 HL2 SIS	17	20
BLA1 CL1 SIS	15	17
BLA1 CL2 SIS	19	21
BLA1 CL3 SIS	19	22
BLA1 CL1 SIS accu	19	24
BLA1 CL2 SIS accu	20	20
BLA1 CL3 SIS accu	18	18
BLA1 HL2 RHR suction	16	20
BLA1 cL2 drain	15	15
BLA1 cL3 drain	15	15
CRU4 CL2 SIS	13	16
CRU4 CL3 SIS	13	16
GOL2 CL4 SIS	12	21

The superposition of these brackets produces the histogram shown in Figure 3-10.

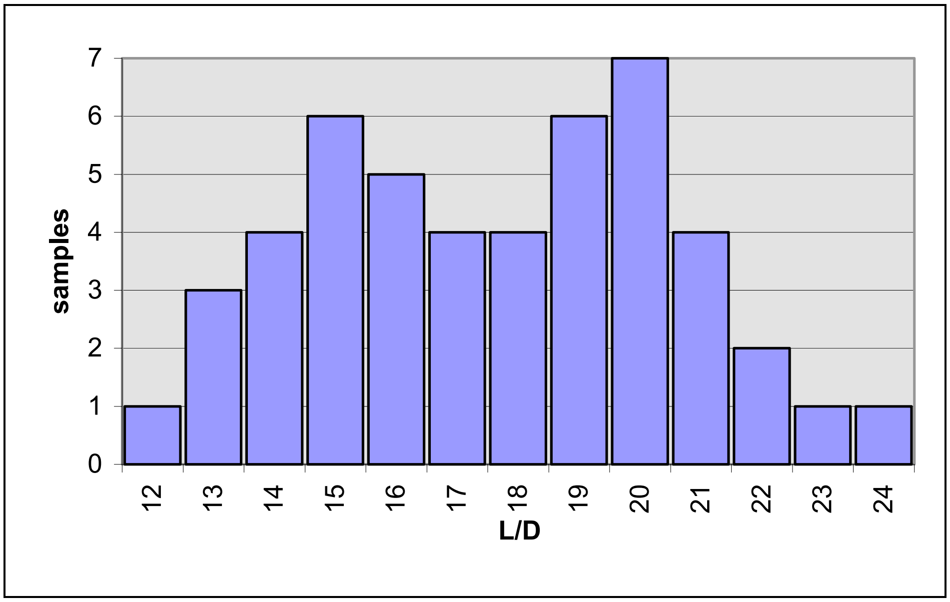

Figure 3-10
Vortex length histogram

The statistical data of this histogram are the following:

- average value of L/D = 17.6

- standard deviation = 2.92

It should be noted that the histogram above does not show the exact position of the vortex phenomenon, but the range in which the phenomenon is observable. Therefore, the extreme values are probably not indicative of vortex fronts and depend on the definition of the instrumentation. Thus, the actual distribution of vortex front lengths is narrower.

The distribution shown above allows one to affirm that the whirl length lies within the range of L/D=14 to L/D=21 in at least 83 % of the cases.

As for the other lines, the vortex length is set by the section valve. In this configuration, the maximum distance between the latter and the primary branch pipe is 16D. Hence, in none of these cases was a vortex exceeding 21D established.

In conclusion, the vortex phenomenon can be observed in all instrumented lines. The penetration varies for every line investigated, independently of its geometry. Instrumentation of dead legs allows us to conclude with near certainty that the vortex length always ranges from 14D to 21D.

3.4.2 Free convection loop and stratification

Appendices A and B show that the phenomenon of free convection was observed in almost all of the instrumented lines.

In many lines, the positioning of the sensors does not allow one to accurately determine the characteristics of the phenomenon and, in particular, the length of the loops.

Unless hindered in its formation by one or two section valves or a vertical downward section, the phenomenon causes very high temperatures to appear at substantial distances from the nozzle, as shown in Table 3-8.

Table 3-8
Examples of high temperatures far from the primary branch

Line Name	L/D	T (°C)
Blayais 1 cL2 drain	144	147
Golfech 2 cL1 drain	139	205
Golfech 2 cL2 drain	140	197

The maximum values of the thermal stratification gradients recorded are shown in Table 3-9.

Table 3-9
Maximum values of the stratification gradients

Line Name	L/D	ΔT (°C)
Dampierre 1 HL1 SIS	26	98
Blayais 1 CL3 SIS accu	24	90
Chinon B3 HL1 SIS	26	80
Golfech 2 HL2 SIS	18	69

Pressure plays an essential role in the appearance of this phenomenon. As an example, in Blayais 1 Cold Leg 1 injection line, when the isolable section is depressurized, natural convection does not take place. In Hot Leg 1 injection line of the same unit, the phenomenon propagates less far in the depressurized state. In both cases, the presence of a two-phase state in the dead-end section confirms that the two-phase state hinders the formation of free convection.

In addition, the tables provided in Appendix A clearly prove that a vertical downward section definitely stops the propagation of heat by natural convection.

In conclusion, this phenomenon contributes to the propagation of the heat in most dead leg lines by relaying the vortex, sometimes over very long stretches. If this phenomenon is not intrinsically harmful, it may become so when combining with other phenomena.

3.4.3 Independent thermal cycling

Table 3-10 contains a summary of the different thermal cycling observed on the entire set of instrumented sections. These thermal cycling correspond to the maximum values measured at 100% NP. The table indicates the line, the sensor name, the corresponding L/D value, the range and pseudo-period of each cycling. This table only reports fluctuations of a range equal to or exceeding 5°C.

Table 3-10
The heaviest thermal cycles at 100% NP

Unit	Line	Sensor	L/D	Amplitude Max (°C)	Pseudo-Period Min (Minutes)(3)
Blayais 1	HL1 SIS	TC 3I	10	9/21 (1)	3
	HL2 SIS	TC 1I	16	11	90
	HL3 SIS	TC 1I	12	9	2
	Cold Leg 2 SIS accu	TC 2S	22	28	20
	Cold Leg 3 SIS accu	TC 2S	21	22	20
	cL2 drain	TC 1	36	10	2
	cL3 drain	TC 1	20	43	2
Cruas 4	Cold Leg 1 SIS	TC 1I	13	11	3
Dampierre 1	Hot Leg 1 SIS	TC 2I	5	6	2-5
		TC 3I	6	9	2-5
		TC 4I	7	10	2-5
		TC 5I	8	12	2-5
		TC 6I	9	15	2-5
		TC 7I	10	21	2-5
		TC 9I (2)	26	20	10
Golfech 2	Cold Leg 1 RHR dis	TC 3I	12	5	2
Fessenheim 1	Cold Leg 1 SIS accu	TC 1I	14	5	20

(1) when the pressure in the common header is in balance with the primary pressure

(2) temperature sensor located in the dead-end section

(3) pseudo-period is the time between two consecutive peaks

The range of these variations is at maximum in the drain line off crossover Leg 3 in Blayais 1. However, it is not the line subject to the highest mechanical loads in so far as its wall-thickness is small.

Additionally, some cycling has been observed during peculiar periods. Indeed, a cycling correlated with exceptional variations in the primary pressure was proven at the level of the lower surface of the dead-end section of the Hot Leg 1 injection line at Blayais 1 (TC 5I and TC 6I). This situation is possible because of the balance of pressure. The fluctuations in temperature remain within a limited range, lower than 10°C. It must be noted that the Hot Leg 2 and 3 injection lines are not affected by this phenomenon which was also proven at Dampierre 1. At the level of TC 9I of this unit, slow thermal variations with a significant maximum range (20°C) were observed, closely correlated with the pressure within the primary coolant loop 2 (Figure 3-8). Due to the lack of information on the pressure values of the other primary legs, this instrumentation has not enabled us to refine our knowledge of the phenomenon involved. However, one may state that wide ranges which are connected to substantial variations in the pressure of loop 2 are rare. Moreover, in the Hot Leg 1 injection line at Blayais 1, more precisely in non-pressurized situations (dead-end section pressure of 3 bar), we observed a thermal cycling during the power decrease to hot shutdown (amplitude 10°C and pseudo-period 10 min) in the lower surface of the dead-end section, which was attributed to a fluctuation of the water – saturated water/steam mixture interface. The occurrence of this phenomenon solely during the pressure decrease to hot shutdown phase was unable to be explained.

A thermomechanical study of the cycling observed at Blayais 1 and Cruas 4 was drawn up for an operation at 100% NP. The stress levels caused by the thermal cycling phenomenon were assessed by means of a mono-dimensional model (auxiliary lines have a thin wall with respect to its diameter). The calculation of the stresses based on temperature measurement was carried out by using Beck's inverse method. This is a sequential minimization method that makes use of the direct problem solution. These calculations were performed on the basis of temperatures measured on the outer skin. They allow one to determine the axial stress of thermal origin. The alternating stress, on the basis of which one can determine the usage factor according to the RCC-M rules (design basis air curves), is then calculated. This calculation is significant only when dealing with slow variations in temperature (frequency lower than 1 Hz). Nonetheless, this simplified calculation serves to obtain a rough estimate of the stress of the inner skin.

This simplified analysis leads to the conclusion that the maximum value of the alternating stress amounts to 67 MPa (Blayais 1, Hot Leg 1 injection line), a value that is far below the endurance limit of the material (180 MPa). As the thermal variations in the other instrumented sections are within the same magnitude, one may state that they do not cause thermal fatigue.

All cases of independent cycling investigated through dead leg instrumentation prove that axial thermal stress is not sufficient to damage a line. The acceptability in terms of mechanical fatigue allows us to conclude that the phenomenon of independent thermal cycling has no harmful effect on the operation of the different lines.

4
HARMFUL PHENOMENA

4.1 Farley-Tihange

The Farley-Tihange phenomenon, so called after the names of the first power plants affected by it, takes place in non-isolable sections. It concerns a deterioration process due to thermal fatigue.

4.1.1 Description

The phenomenon is likely to appear in any auxiliary line connected to a pump discharging under normal operating conditions. In French units, this concerns theoretically all of the safety injection lines in the hot and cold legs of 900 MW units (except the accumulator injection lines) and the auxiliary spray lines of all units.

It has led to a great number of incidents throughout the world, in units of various design. In France, three class 1 incidents have been ascribed to this phenomenon in hot leg safety injection lines. Studies were carried out on this subject and have made it possible to characterize the phenomenon as follows.

The high-pressure safety injection is performed by the charging pumps (CVC). The motorized or manually operated wedge gate valves isolating the SIS lines from the CVC system must withstand a pump discharge pressure of 180 bar. The RCS pressure being 155 bar, the non-tightness of either of these valves leads to the appearance of a thin cold water stream along the lower surface of the non-isolable section, so that a thermal stratification zone is created (zone 3 of Figure 4-1). The thin cold water stream meets with the hot water vortex; this is the clash zone (zone 2), the location of which depends on the cold water flow rate. In this zone 2, when the cold water comes in contact with the pipe, the temperature of the metal decreases. Then the water conveyed by the vortex chases the cold water and heats the wall. Therefore, the vortex loses part of its energy and is no longer capable of bringing along the thin cold water stream, so that the latter will flow again. When the energy brought in by the primary fluid becomes preponderant anew, the cycle will take place again.

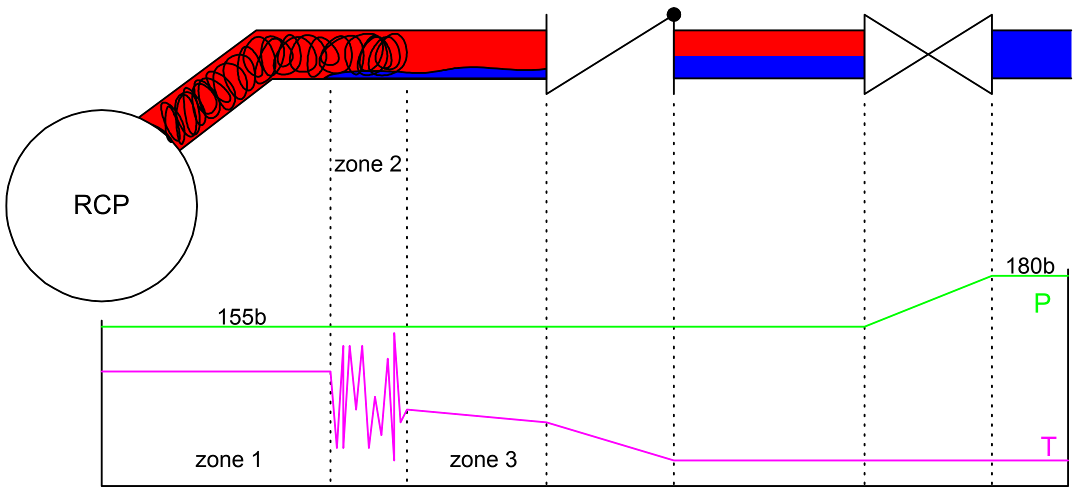

Figure 4-1
Diagram of the Farley-Tihange phenomenon

Thus, the wall metal undergoes a thermal cycle that leads to substantial periodic mechanical stresses along the lower pipe surface. Consequently, there is a risk of primary fluid leakage that cannot be isolated when a through-wall crack appears.

Within the scope of the studies aimed at explaining the causes of the phenomenon, the instrumentation of the Blayais 1 unit was subject to special tests which are analyzed hereinafter.

4.1.2 Injection tests

These tests were discussed earlier in section 2.6.1. It should be noted that they consist of simulating a known leakage flow of an HHSI section valve while recording the temperatures at the outer surface of the SIS lines. This test array makes it possible to adjust stable flow levels within a flow rate range from 10 to 300 l/h and accurately meter the flow rates set. (Note that, downstream of the injection point, the flow splits into three separate lines. Leakage flows in these individual lines was not measured. However, based on temperature measurements on the three lines, it was determined that significant flow occurred only in Line 1. It is not understood why the leakage occurred in only one line.)

The initial thermal state of the three lines is hardly different from the one presented on pages A-2 to A-4, with the operating characteristic stabilized at 100% NP. Before the test was started, thermal cycling could be observed in line 3 only. The characteristics of this cycling are detailed below (Table 4-1).

For each of the injection flow rates, during stabilized periods, we have calculated the average value of the temperatures measured during 10 minutes. The results obtained enable us to trace the curves provided in Appendix C. These are the conclusions that can be drawn from these curves (C-1 to C-7):

- Line 1 is the seat of a temperature change as soon as the minimum injection flow is reached. The decrease in temperature up to the primary branch pipe allows one to affirm that the cold water flow is initiated at a flow rate of 10 l/h (Figure C-1). At a flow rate of over 70 l/h, the temperature of the lower pipe surface upstream of the check valve becomes close to the temperature of the vertical section. Notice that there is a characteristic flow rate around 30 l/h that corresponds to the maximum stratification within the horizontal section upstream of the check valve RCP 120 VP (Figure C-7).

- Line 2, throughout the test series, experiences almost no variation of thermal loads, whatever the injection flow rate. Only the thermocouples located next to the vertical elbow detect a very slight variation.
- In line 3, there is no variation in thermal loads up to a flow rate of 299 l/h; beyond this value, further testing revealed a slight increase in thermal loads.
- Except for line 2, the thermal loads are not exactly the same at the end of injection as those measured before the start of injection, even if they are close.

Development of thermal cycling

- Leg 1

In the test, the thermal state downstream of the check valve is characterized by the following parameters:

- average stratification: difference in temperature between the upper and lower pipe surfaces for the thermal loads previously described
- maximum stratification: maximum difference in temperature between the upper and lower pipe surfaces
- maximum range: maximum range from peak to peak of thermal cycling along the lower pipe surface
- pseudo-period: estimation of the average period of thermal cycling over a time of 30 min
- maximum gradient: maximum slope of thermal cycling

As no variation exceeding 5 °C was found along the upper pipe surface, further investigations were exclusively focused on the fluctuations along the lower pipe surface. Table 4-1 summarizes the characteristics of thermal cycling depending on the steady flow rate injected:

Table 4-1
Characteristics of thermal cycling depending on the flow rate injected

Flow Rate	Location In LG	Average Stratification	Maximum Stratification	Maximum Amplitude	Pseudo-Period [(1)]	Maximum Gradient
l/h	°C	°C	°C	°C	minute	°C/min
0	BC1 TC 1I	8	10	1		
	BC1 TC 2I	1	1	1		
	BC1 TC 3I	15	20	16	1,5	10
10	BC1 TC 1I	8	8	1,5		
	BC1 TC 2I	1	1	7		8
	BC1 TC 3I	56	60	25	1	20
30	BC1 TC 1I	8	10	2		
	BC1 TC 2I	5	20	15	2	10
	BC1 TC 3I	88	92	15	1	2
70	BC1 TC 1I	8	8	2		
	BC1 TC 2I	10	30	28	1	28
	BC1 TC 3I	106	110	5		
120	BC1 TC 1I	8	8	2		
	BC1 TC 2I	28	55	40	1	50
	BC1 TC 3I	121	125	5	1	3
170	BC1 TC 1I	9	10	2		
	BC1 TC 2I	48	70	46	1	60
	BC1 TC 3I	133	140	8		
277	BC1 TC 1I	10	12	3		
	BC1 TC 2I	69	98	50	1	53
	BC1 TC 3I	155	155	6		
299	BC1 TC 1I	10	12	3		
	BC1 TC 2I	85	105	68	1	70
	BC1 TC 3I	152	160	7		
101	BC1 TC 1I	8	10	2		
	BC1 TC 2I	21	40	35	1	30
	BC1 TC 3I	114	120	15	1	5
70	BC1 TC 1I	8	10	1,5		
	BC1 TC 2I	12	25	23	1	25
	BC1 TC 3I	104	105	5		
5	BC1 TC 1I	8	10	1		
	BC1 TC 2I	2	6	4		
	BC1 TC 3I	57	70	34	1	20
0	BC1 TC 1I	8	10	1		
	BC1 TC 2I	1	5	3	1	4
	BC1 TC 3I	21	30	20	1	20

[(1)] Pseudo-period is the time between two consecutive peaks.

The principal effects of the injection flow rate on thermal cycling are:

- a variation of the range of the phenomenon which increases as the injection flow rate increases. It amounts to 68 °C from peak to peak at a flow rate of 299 l/h.
- a change of the phenomenon that leads to a shift of the maximum range zone of cycling along the line, when the flow rate varies.

Indeed, for a zero injection flow rate, the maximum range is measured in section 3, directly downstream of the check valve RCP 120 VP. For a flow rate of 30 l/h and above, the maximum range is measured in section 2, next to the elbow located downstream of the check valve.

Given the positions of the thermocouples, nothing allows us to affirm that we have detected the maximum range of the phenomenon.

- Leg 2

No cycling appears.

- Leg 3

No cycling appears.

Figure 4-2 shows the development of thermal cycling during the test:

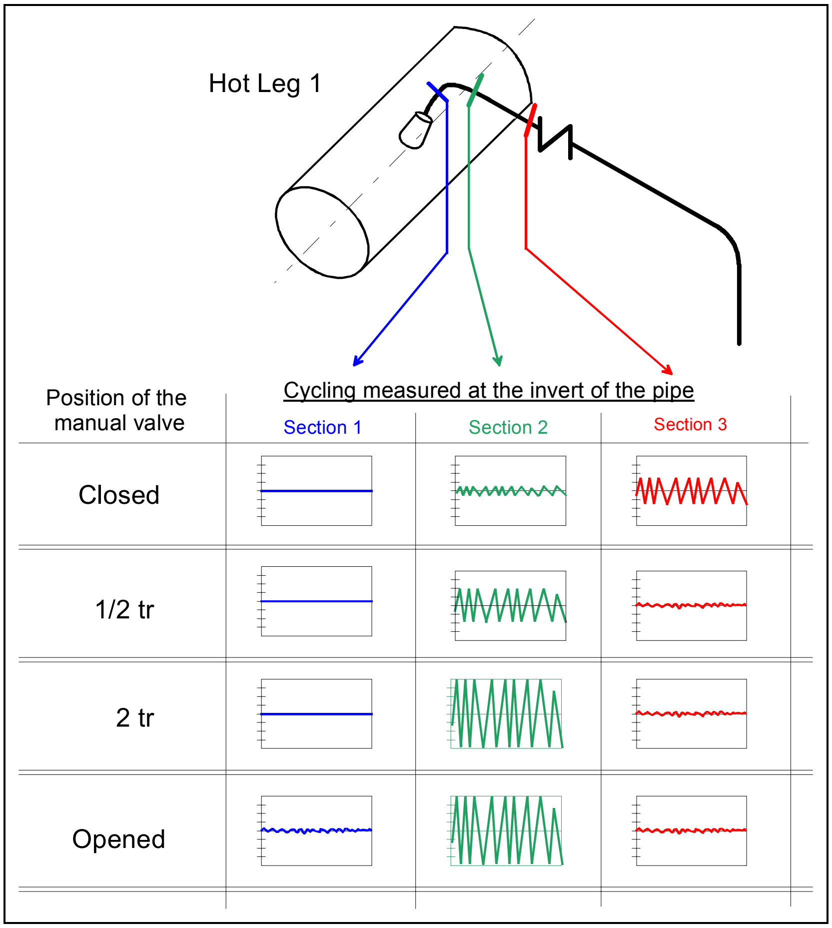

Figure 4-2
Development of thermal cycling during the injection test

The injection tests have allowed us to characterize the thermal fluctuations caused by valve leakage. In addition, the mechanical analysis of the non-isolable section of the line has shown that:

- the thermal fluctuations that take place downstream of the check valve at an injection flow rate equal to zero do not cause any deterioration of the line.

- the maximum permissible injection flow rate taking into account the thermal fatigue risk amounts to 100 l/h.

4.1.3 Conclusion

The studies carried out by EDF and the instrumentation implemented have provided us with a good knowledge of the Farley-Tihange phenomenon.

However, double cracking at Dampierre 1 in 1997 was especially surprising by its location in the straight part of the pipe. It mainly showed that our knowledge of the phenomena was still imperfect. Until then, the welds had always been regarded as the most sensitive points of the auxiliary lines. In fact, the interaction between the primary vortex and the cold water leakage is very local and the instrumentation of Blayais 1 did not make it possible to extrapolate the results obtained at the two ends of the horizontal pipe to the straight part of the line.

Among the investigations carried out following the discovery of the cracks, temperature measurements during hot shutdown on the damaged line allowed us, by comparison with Blayais 1 injection tests data, to identify the origin of the problem as being the SIS/CVC isolation valve leakage. While waiting for the generalization of a modification equivalent to that of Tihange (pressure well), these temperature measurements are now carried out during each start-up of the reactor with the objective of highlighting a possible cold water leakage.

The instrumentation of Dampierre 1 was installed on the SIS line in hot leg 1 in order to improve our knowledge in the zone in question and to compare, to a greater extent, the line loads with those of Blayais 1. The valve separating the SIS and CVC circuits have been repaired. This instrumentation showed that, in the absence of leakage, thermal loads are equivalent between the two units.

4.2 Vortex instability

In this section we deal with a phenomenon that, unlike the Farley-Tihange phenomenon, has not caused any incident in France. However, a number of incidents throughout the world are partially ascribed to this phenomenon.

4.2.1 Description

When the vortex is located in a downward vertical section, the thermohydraulic configuration is unstable. This is due to the fact that the forced convection imposed by the vortex, which tends to transmit the heat downwards, clashes with the density effects.

This has been proven by means of the instrumentation set up in Blayais 1 on the Cold Leg 3 injection line (Figure 4-3). Cooling down of section 3 located in the straight line portion downstream of the check valve RCP 322 VP is followed by rapid heating. The maximum thermal characteristics are the following:

- ΔT_{max} = 60 °C (local cooling range)
- $\Delta T / \Delta t_{max}$ = 0.5 °C / min (cooling)
- $\Delta T / \Delta t_{max}$ = 7 °C / min (heating)
- pseudo-period: variable over the cycle
- maximum frequency of appearance: 3 / day

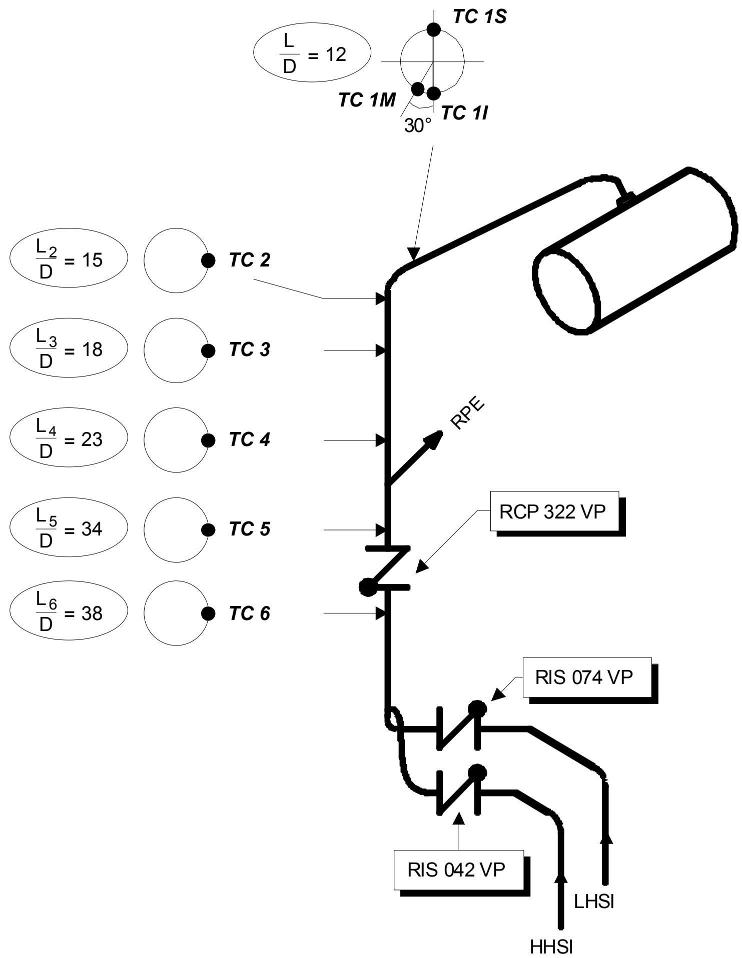

Figure 4-3
Blayais 1 Cold Leg 3 injection line

The phenomenon showed itself in a random (or pseudo-random) manner during normal operating modes at 100-percent power in the way described as follows: in parallel to the cooling-down of a part of the vertical section downstream of the check valve RCP 322 VP, followed by rapid heating, one observes slight warming by about 5 °C of the branch pipe (TC1I, TC1M and TC2). The time of occurrence of the phenomenon is totally random. Cooling is ascribed to slow retreat of the vortex in the vertical section towards the branch, thus causing slight warming in the branch area. It should be noted that cooling and warming kinetics are different. The line cools down slowly (this process lasts approximately two hours) by natural conduction to the ambient external milieu, whilst the heating initiated by vortex withdrawal is faster due to forced convection. This phenomenon is shown in Figure 4-4.

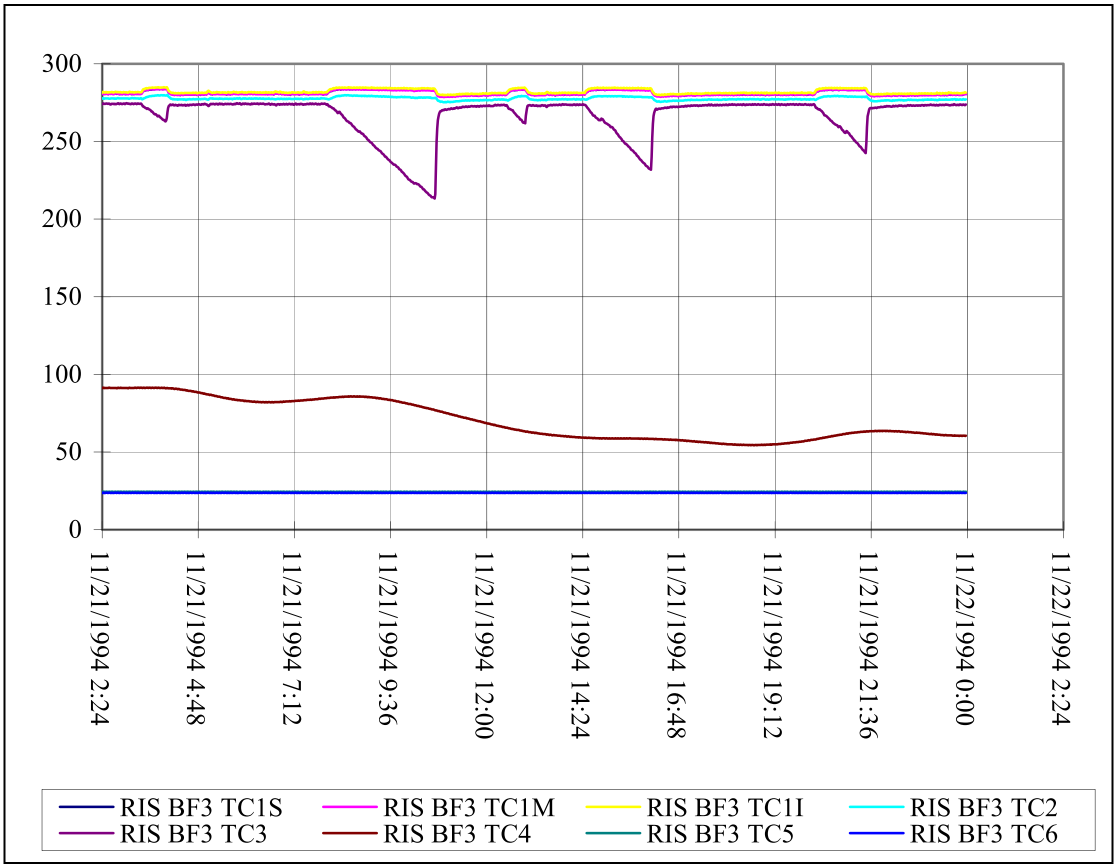

Figure 4-4
Thermal transients on Blayais 1 Cold Leg 1 injection line (°C)

The mechanical calculations performed on this type of transient state (mono-dimensional) show that the axial stress remains far below the fatigue limit of the material (180 MPa).

However, this instability may have a greater impact when the vertical section is followed by a horizontal section and when the vortex is located within the elbow zone. Such a case was found in the Cold Leg 3 accumulator injection line of the same unit (Figure 4-5). Heating occurred in the horizontal section downstream of check valve RCP 321 VP and to a greater extent along the upper pipe surface (TC 2S). The phenomenon is shown in Figure 3-7. The maximum thermal characteristics of this case are as follows:

- ΔT_{max} = 120 °C (heating range)
- $\Delta T / \Delta t_{max}$ = 25 °C / min
- pseudo-period: variable over the cycle
- maximum frequency of appearance: 3 / day
- heating time: approximately two hours

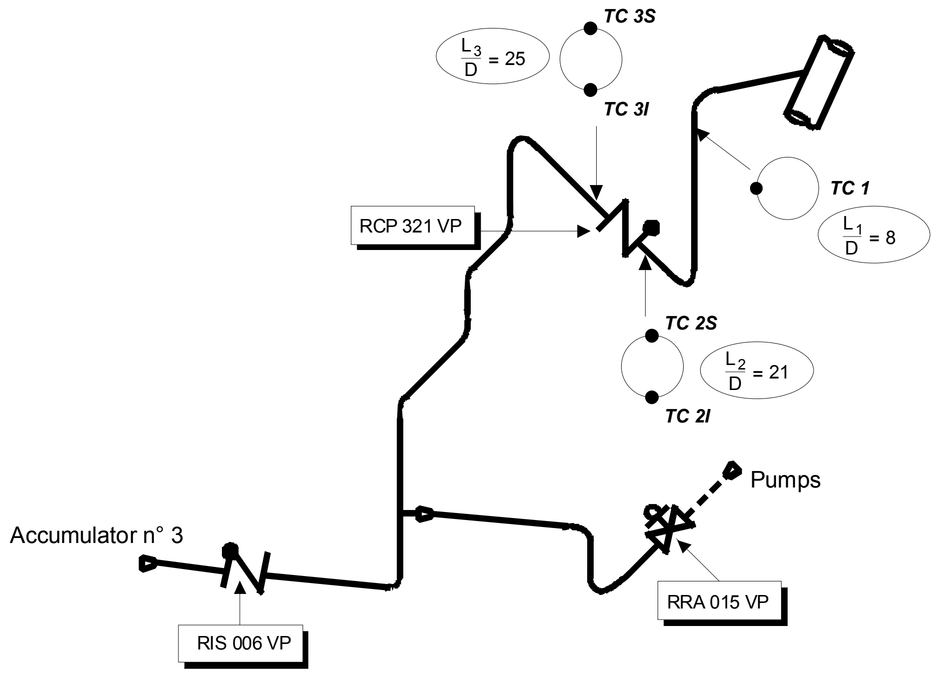

Figure 4-5
Cold Leg 3 accumulator injection line

This localized heating phenomenon appeared about ten days after criticality while an overall cooling-down of sections 2 and 3 was observed. From this day on, it showed itself in a random way, whatever the boiler operating mode (power on or shutdown), in a nearly instantaneous temperature increase along the upper pipe surface of section 2 (by 100 to 130 °C) and, as for section 3, in a temperature increase which took place at a slower pace and remained within a less wide range (by 70°C). The lower pipe surfaces of these sections are also affected by the increase in temperature, but with a delay of 2 hours and a range three times smaller. As of mid-October 1994, overall heating of the line occurred and the frequency of occurrence of the phenomenon increased without any obvious cause, thereby preventing the line from cooling down. The range of the transient states in fact diminished; from late January 1995 until the shutdown of the unit in June 1995, the line's thermal load remained globally high and stable without any fluctuation.

This warming is ascribed to an increase in the penetration depth of the primary vortex in the vertical section of the line. As set forth in Section 3, the flow is split up into two streams, a hot penetrating one and a colder stream that goes up to the branch point. As for this particular line, the vortex resides most probably in the elbow zone. This causes a hot water stream to be propagated along the upper surface of the horizontal line portion located downstream of the check valve RCP 321 VP. At the same time, a slight cooling by 10°C is observed in the branch point area; this can be interpreted as resulting from the return of the cold water swept back by the advance of the vortex.

4.2.2 Conclusion

Up to the present time, the driving factors causing this phenomenon to appear have not been fully identified.

The mechanical calculations of the most loaded zone (section 2 of Cold Leg 3 accumulator injection line) were performed in compliance with the RCC-M rules. The results reveal a usage factor that remains below 1 over a 40-year period.

Any auxiliary line which includes a vertical downward section and then continues as a horizontal section is likely to be affected by this phenomenon. However, it is difficult to forecast its appearance, given that the latter depends upon the vortex position with respect to the elbow, which may be variable, even in identical units.

A
DATA EVALUATION

See Sections 2 and 3 for a description of the data presented in Appendix A.

The following comments refer to annotations on the figures in this Appendix:

- a1: temperature level, stratification amplitude and cycling enable to determine the presence of the vortex.

- a2: free convection is likely to occur in this section even if it is limited by two-phase state (not represented in that case).

- a3: the thermal fluctuations (lower pipe surface) result from the interaction between the whirl and the convection loop. Therefore, stratification and cycling amplitudes allow to conclude that the vortex reach this section.

- a4: in this section, cycling amplitude is 4 °C.

- a5: for any vertical downward line followed by a horizontal one, when cycling is noticed along the upper pipe surface, we assess that the vortex front is located in the elbow zone.

- a6: this instrumentation detected thermal fluctuations from the beginning of the non-isolable section to the first valve (reached by the vortex). On the other lines, the geometry of which is identical (Hot Leg 1 injection line of Blayais 1 and Chinon B3), there is only a cycling for Blayais 1, close to the valve. This difference may be explained by the thermohydraulics phenomena behavior changing from one unit to another and by the fact that the number and the position of the sensors are always different.

SPS : CPY	***Line : BLAYAIS 1*** Hot Leg 1 injection line							
section	S1	S2	S3 (a1)		S4 (a2)	S5	S6	S7
L/D	2	5	10		15	26	27	28
pressure	155				5 155			
	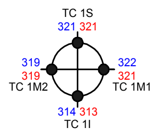	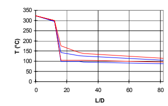	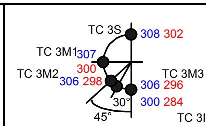	Check Valve RCP 120 VP	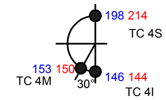	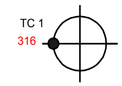	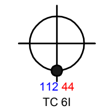	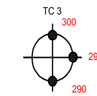
orientation	IU	H	H	H	H	H	VE	VD
insulation								
vortex								
free convection loop								
stratification	7 8	0 1	8 18		52 70	1 79		
diphasic state					X			
cycling			LG LG					
geometry	6" schedule 160				6" schedule 160			
primary temperature T_{HL} = 323 °C					*primary flow rate* Q_{RCS} = 22250 m^3/h			

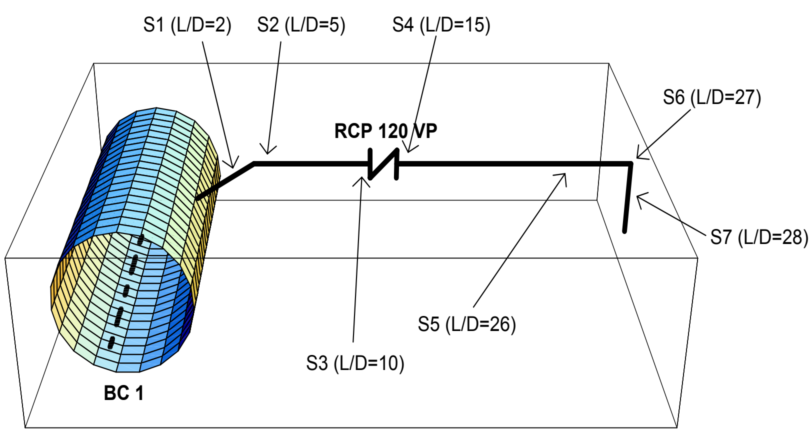

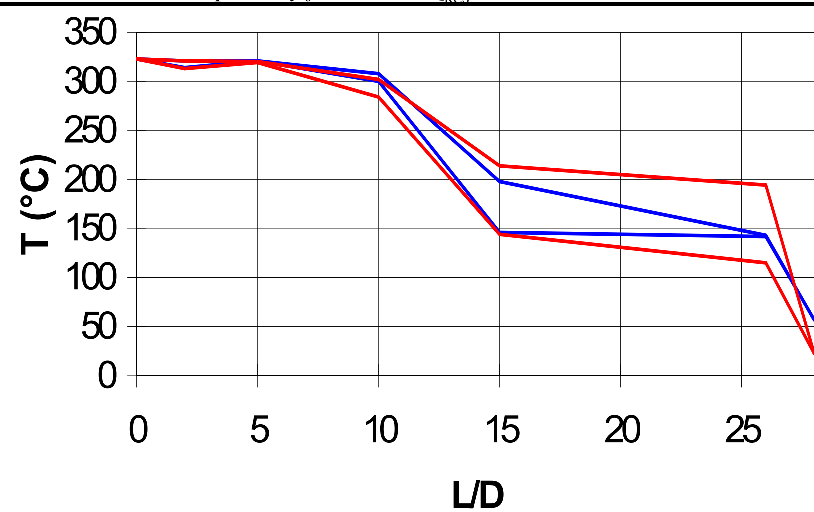

Red / Blue: measurements that correspond to periods of different thermal loadings

SPS : CPY	***Line : BLAYAIS 1*** Hot Leg 2 injection line							
section	S1 (a3)	S2	S3		S4	S5	S6	S7
L/D	16	21	26		31	33	74	77
pressure	155				5 155			
	TC 1S 302 302 / 273 275 TC 1I	TC 2S 302 302 / 272 272 TC 2I	TC 3S 301 301 / 263 265 TC 3I	Check Valve RCP 220 VP	TC 4S 166 195 / 115 119 TC 4I	TC 5S 141 168 / 106 110 TC 5I	TC 6S 126 130 / 103 109 TC 6I	TC 7 52 79
orientation	H	H	H	H	H	H	H	VD
insulation								
vortex								
free convection loop								
stratification	29 27	30 30	38 36		51 76	35 58	23 21	
diphasic state					X			
cycling	LG LG							
geometry	6" schedule 160				6" schedule 160			
primary temperature T_{HL} = 323 °C				*primary flow rate* Q_{RCS} = 22250 m^3/h				

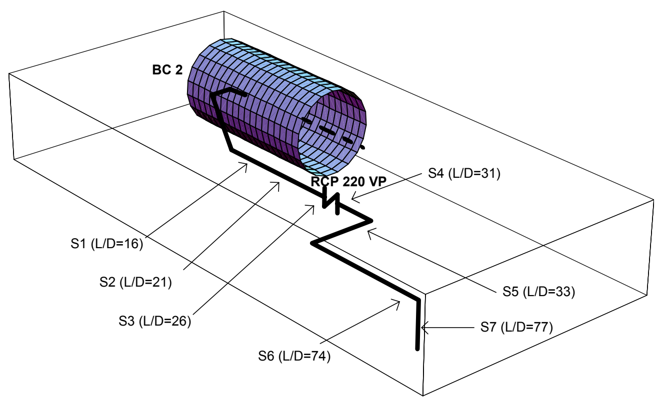

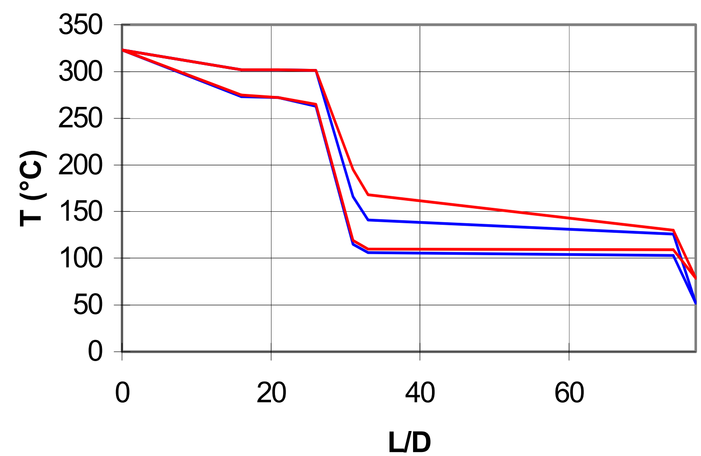

Red / Blue: measurements that correspond to periods of different thermal loadings

SPS : CPY	***Line : BLAYAIS 1*** Hot Leg 3 injection line					
section	S1		S2	S3	S4	S5
L/D	12		16	28	31	82
pressure	155		5 155			
	TC 1S 296 299 / 297 300 TC 1I	Check Valve RCP 320 VP	TC 2S 143 175 / 98 105 TC 2I	TC 3S 126 142 / 99 106 TC 3I	TC 4S 125 138 / 96 104 TC 4I	TC 5S 106 114 / 87 96 TC 5I
orientation	H	H	H	H	H	H
insulation						
vortex						
free convection loop						
stratification	-1 -1		45 70	27 36	29 34	19 18
diphasic state						
cycling	LG LG					
geometry	6” schedule 160		6” schedule 160			
primary temperature T_{HL} = 323 °C			*primary flow rate* Q_{RCS} = 22250 m^3/h			

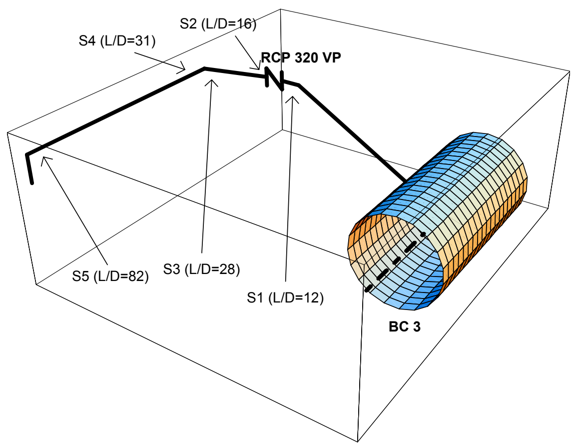

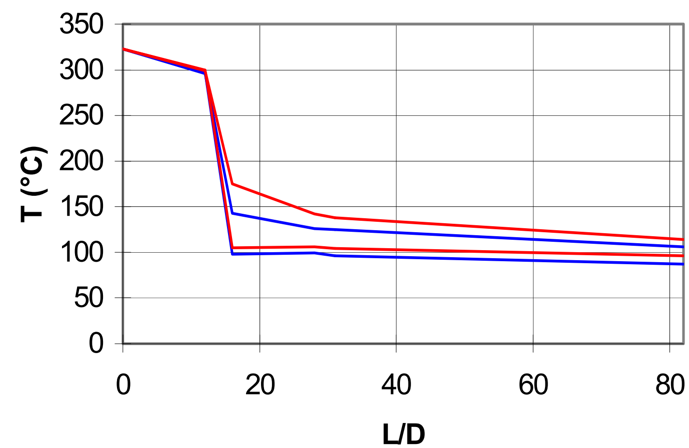

Red / Blue: measurements that correspond to periods of different thermal loadings

SPS : CPY	***Line : BLAYAIS 1*** Hot Leg 2 RHR Suction								
section	S1	S2	S3 (a3)	S4	S7		S5		S6
L/D	12	14	15	21	23		25		31
pressure	155						155		3
	TC 1 316	TC 2 312	TC 3 300 294 290	TC 4 292 275	TC 7 295 274	Gate Valve RCP 215 VP	TC 5 182 126	Gate Valve RRA 021 VP	TC 6 102 81
orientation	VD	VD	H	H	H	H	H	H	H
insulation									
vortex									
free convection loop									
stratification			10	17	21		56		21
diphasic state									
cycling			LG (a4)						
geometry	14” schedule 140						14” sch. 140		14” sch. 140
primary temperature T_{HL} = 323 °C					*primary flow rate* Q_{RCS} = 22250 m^3/h				

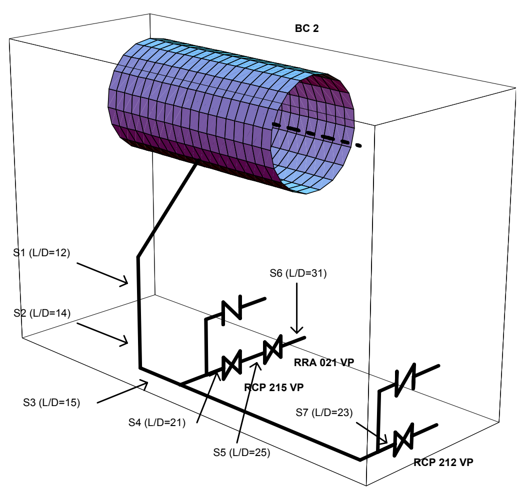

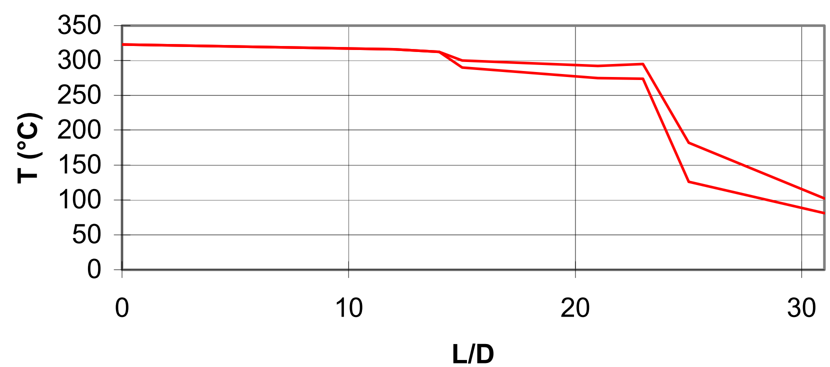

SPS : CPY	***Line : BLAYAIS 1*** Draining of the crossover Leg 2			
section	S1 (a5)	S2		S3
L/D	36	144		175
pressure	155			?
	TC 1 184	TC 2 147	Gate Valve RCP 213 VP	TC 3 63
orientation	H	H	H	H
insulation				?
vortex				
free convection loop				
stratification				
diphasic state				
cycling	UG			
geometry	2" schedule 160			¾" schedule 160
primary temperature T_{cL} = 286 °C		*primary flow rate* Q_{RCS} = 22250 m^3/h		

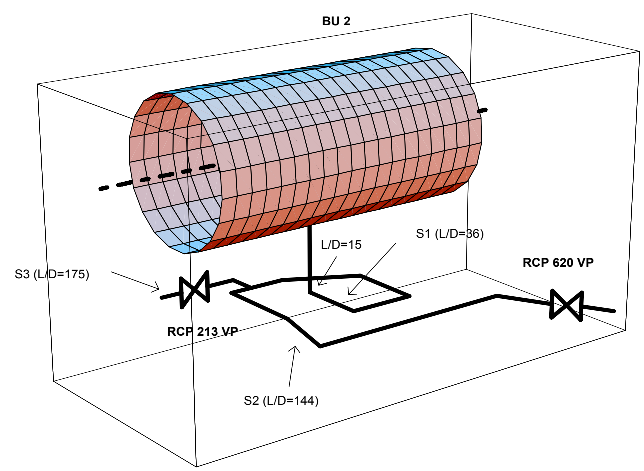

NB : no insulation beyond RCP 620 VP

SPS : CPY	***Line : BLAYAIS 1*** Draining of the crossover Leg 3			
section	S1 (a5)	S2		S3
L/D	20	168		280
pressure	155			
	TC 1 187	TC 2 25	Gate Valve RCP 630 VP	TC 3 24
orientation	H	H	H	H
insulation				
vortex				
free convection loop				
stratification				
diphasic state				
cycling	UG			
geometry	2" schedule 160			2" schedule 160
primary temperature T_{cL} = 286 °C		*primary flow rate* Q_{RCS} = 22250 m^3/h		

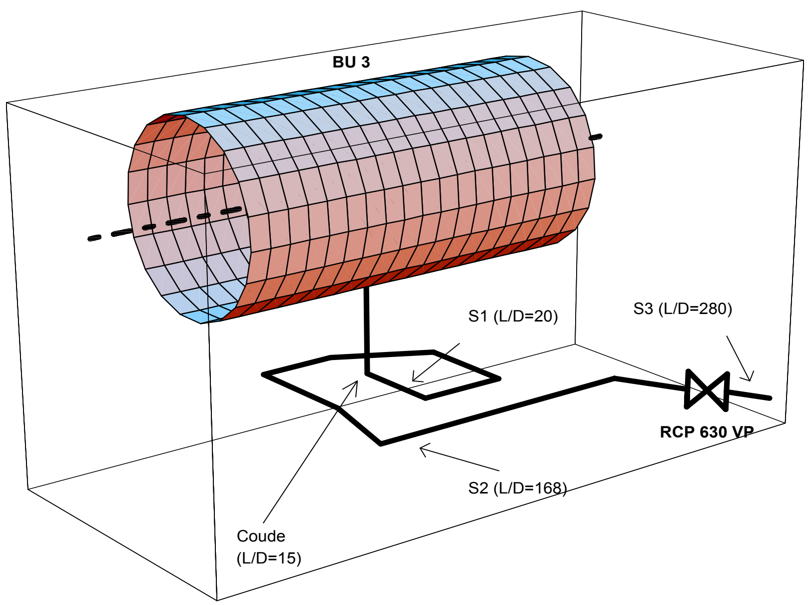

SPS : CPY	***Line : DAMPIERRE 1*** Hot Leg 1 injection line (a6)									
section	S1	S2	S3	S4	S5	S6	S7		S8	S9
L/D	4	5	6	7	8	9	10		15	26
pressure	155								155 155	
	321 319 TC 1I	317 314 TC 2I	313 309 TC 3I	314 309 TC 4I	311 305 TC 5I	305 296 TC 6I	308 304 TC 7S 305 290 TC 7I	Check Valve RCP 120 VP	222 213 TC 8S 160 130 TC 8I	200 188 TC 9S 135 90 TC 9I
orientation	H	H	H	H	H	H	H	H	H	H
insulation										
vortex										
free convection loop										
stratification							3 14		62 83	65 98
diphasic state										
cycling	LG LG	LG LG	LG LG	LG LG	LG LG	LG LG	LG LG			LG LG
geometry	6" schedule 160								6" schedule 160	
primary temperature T_{HL} = 323 °C					*primary flow rate* Q_{RCS} = 22250 m^3/h					

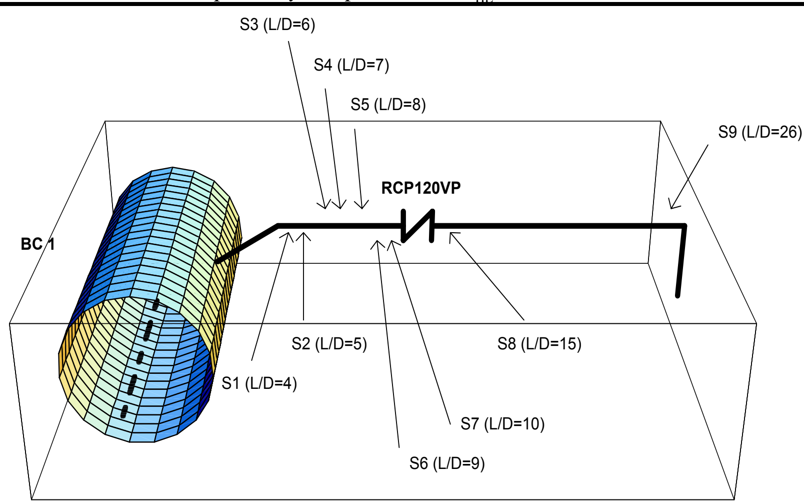

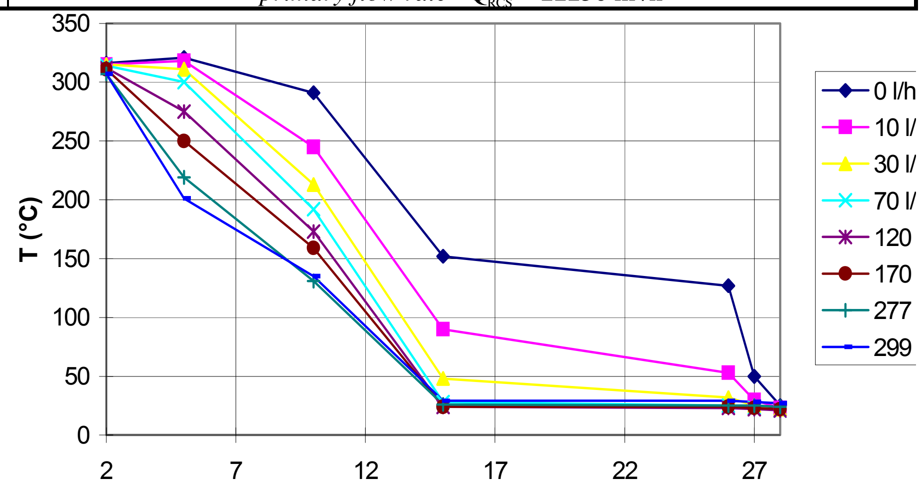

Red / Blue: measurements that correspond to periods of different thermal loadings

B
GENERIC THERMOHYDRAULIC PHENOMENA

See Section 3.4 for a description of the charts in this appendix,

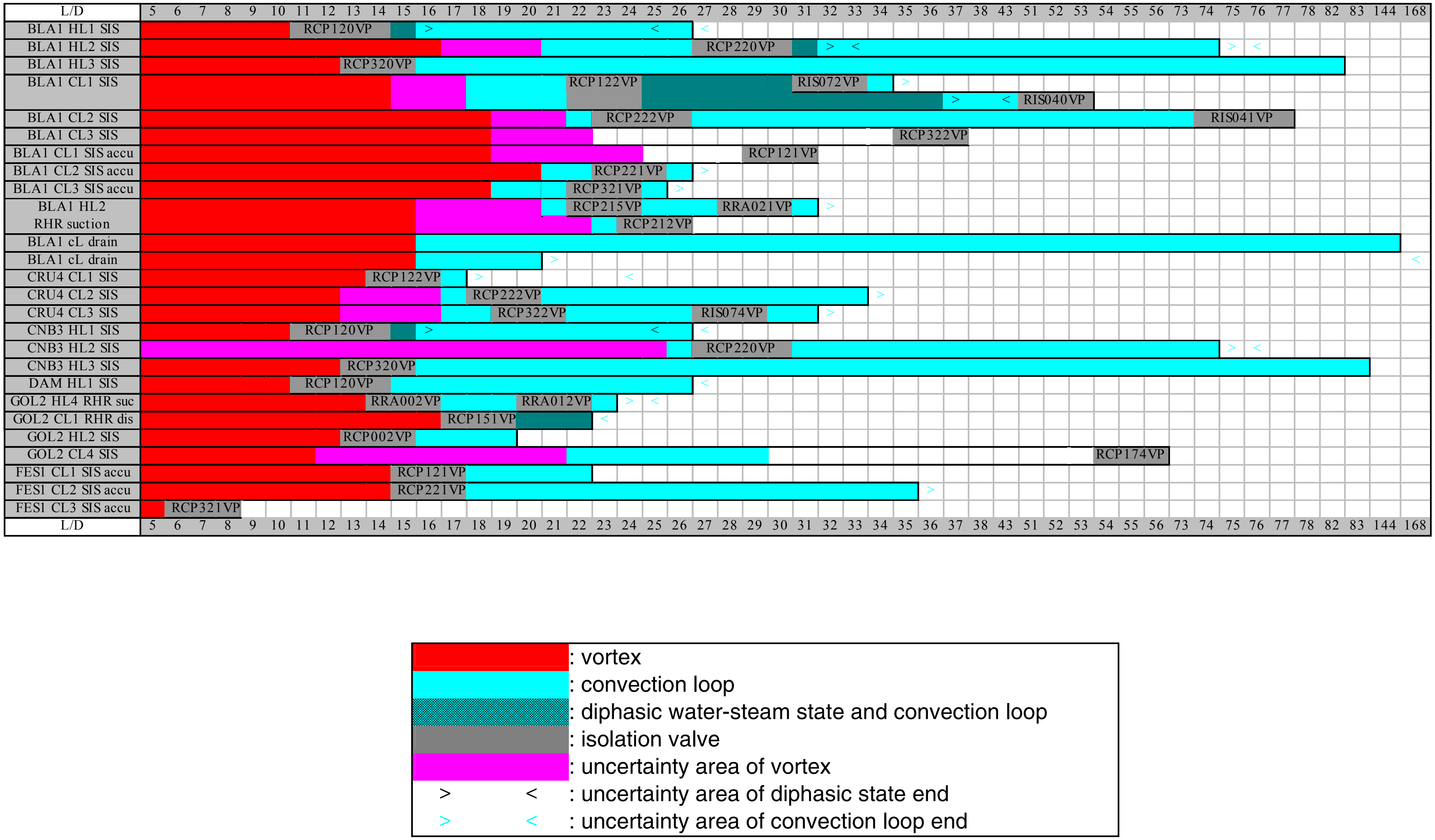
L/D
5 6 7 8 9 10 11 12 13 14 15 16 17 18 19 20 21 22 23 24 25 26 27 28 29 30 31 32 33 34 35 36 37 38 43 51 52 53 54 55 56 73 74 75 76 77 78 82 83 144 168
BLA1 HL1 SIS
RCP120VP
BLA1 HL2 SIS
RCP220VP
BLA1 HL3 SIS
RCP320VP
BLA1 CL1 SIS
RCP122VP
RIS072VP
RIS040VP
BLA1 CL2 SIS
RCP222VP
RIS041VP
BLA1 CL3 SIS
RCP322VP
BLA1 CL1 SIS accu
RCP121VP
BLA1 CL2 SIS accu
RCP221VP
BLA1 CL3 SIS accu
RCP321VP
BLA1 HL2 RHR suction
RCP215VP
RRA021VP
RCP212VP
BLA1 cL drain
BLA1 cL drain
CRU4 CL1 SIS
RCP122VP
CRU4 CL2 SIS
RCP222VP
CRU4 CL3 SIS
RCP322VP
RIS074VP
CNB3 HL1 SIS
RCP120VP
CNB3 HL2 SIS
RCP220VP
CNB3 HL3 SIS
RCP320VP
DAM HL1 SIS
RCP120VP
GOL2 HL4 RHR suc
RRA002VP
RRA012VP
GOL2 CL1 RHR dis
RCP151VP
GOL2 HL2 SIS
RCP002VP
GOL2 CL4 SIS
RCP174VP
FES1 CL1 SIS accu
RCP121VP
FES1 CL2 SIS accu
RCP221VP
FES1 CL3 SIS accu
RCP321VP
: vortex
: convection loop
: diphasic water-steam state and convection loop
: isolation valve
: uncertainty area of vortex
> < : uncertainty area of diphasic state end
> < : uncertainty area of convection loop end

C
INJECTION TESTS ANALYSES

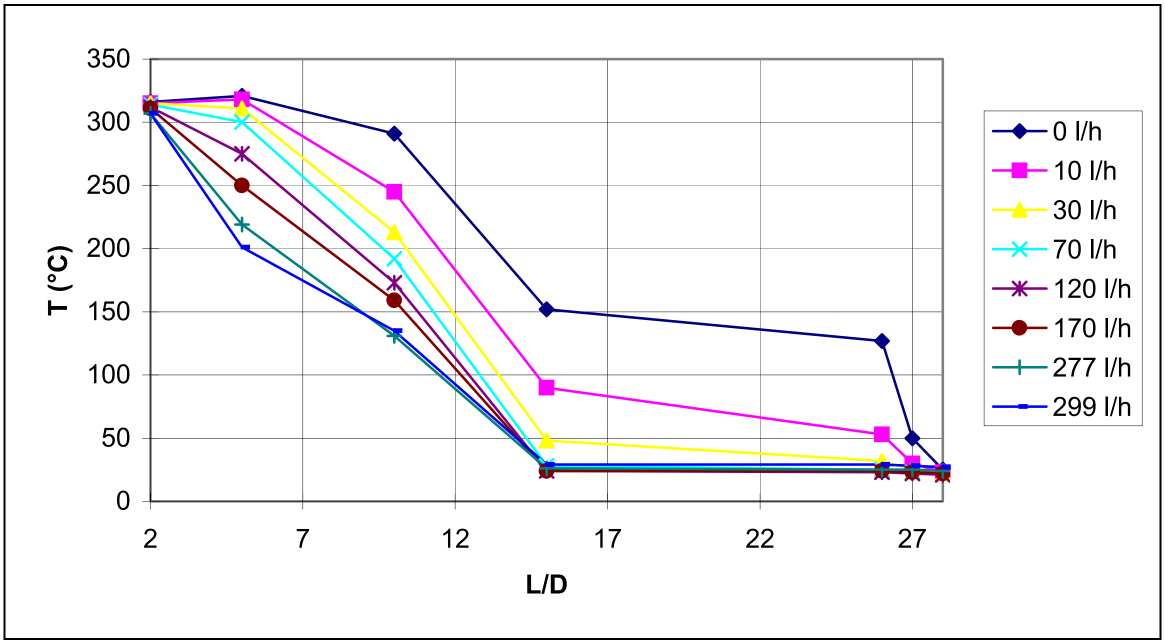

Figure C-1
Hot Leg 1 injection test (0-300 l/h)

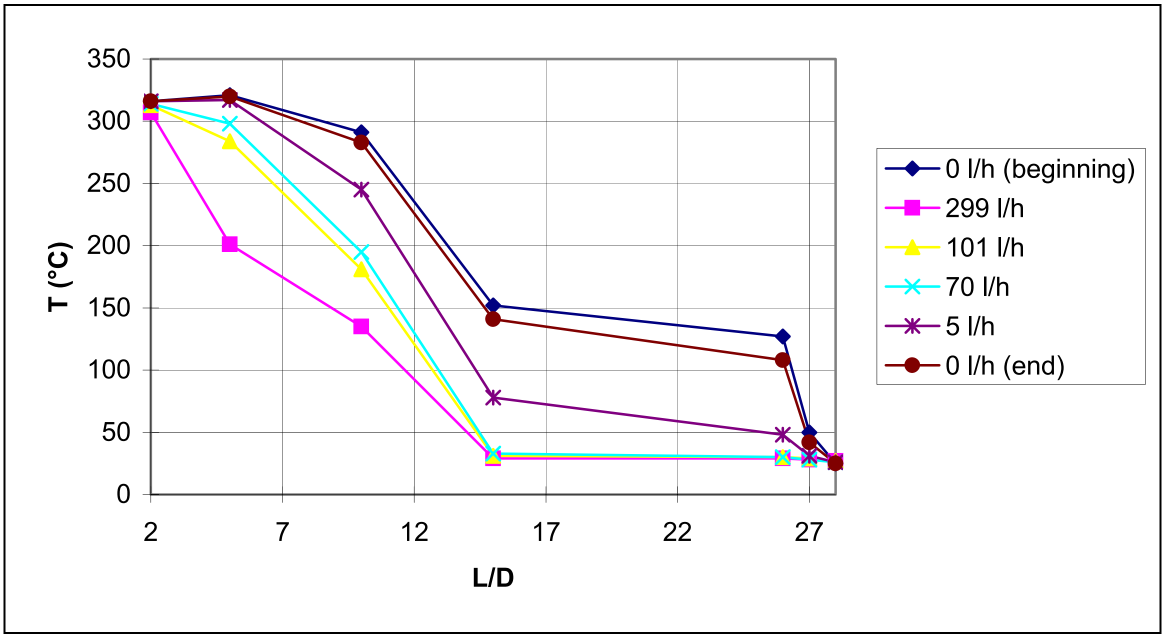

Figure C-2
Hot Leg 1 injection tests (300-0 l/h)

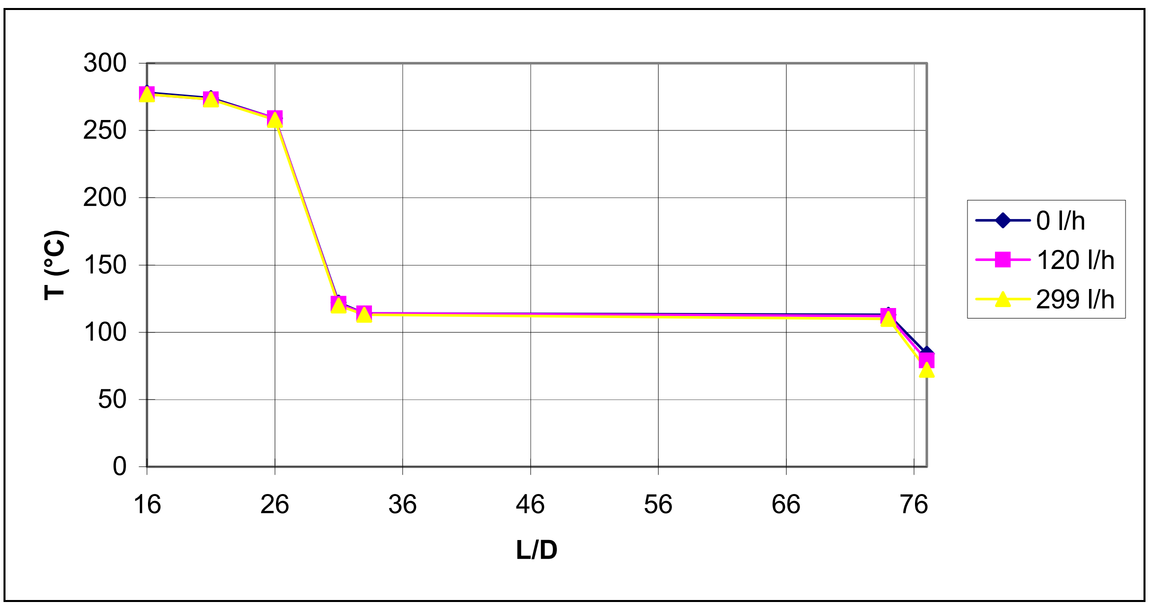

Figure C-3
Hot Leg 2 injection tests (0-300 l :h)

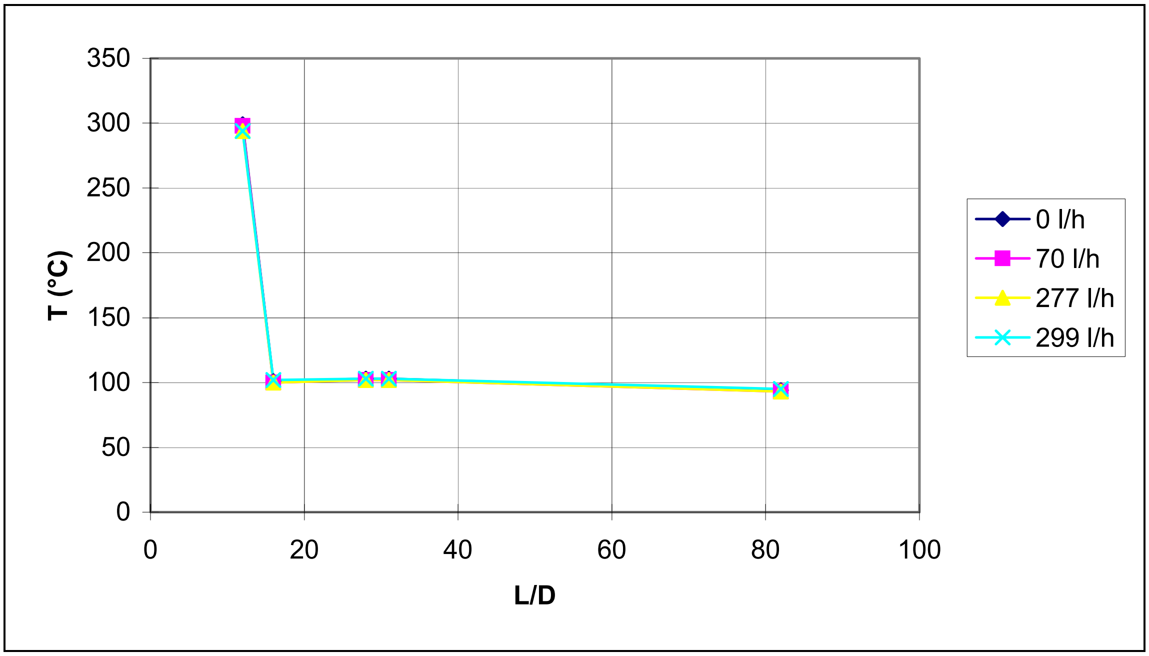

Figure C-4
Hot Leg 3 injection tests (0-300 l/h)

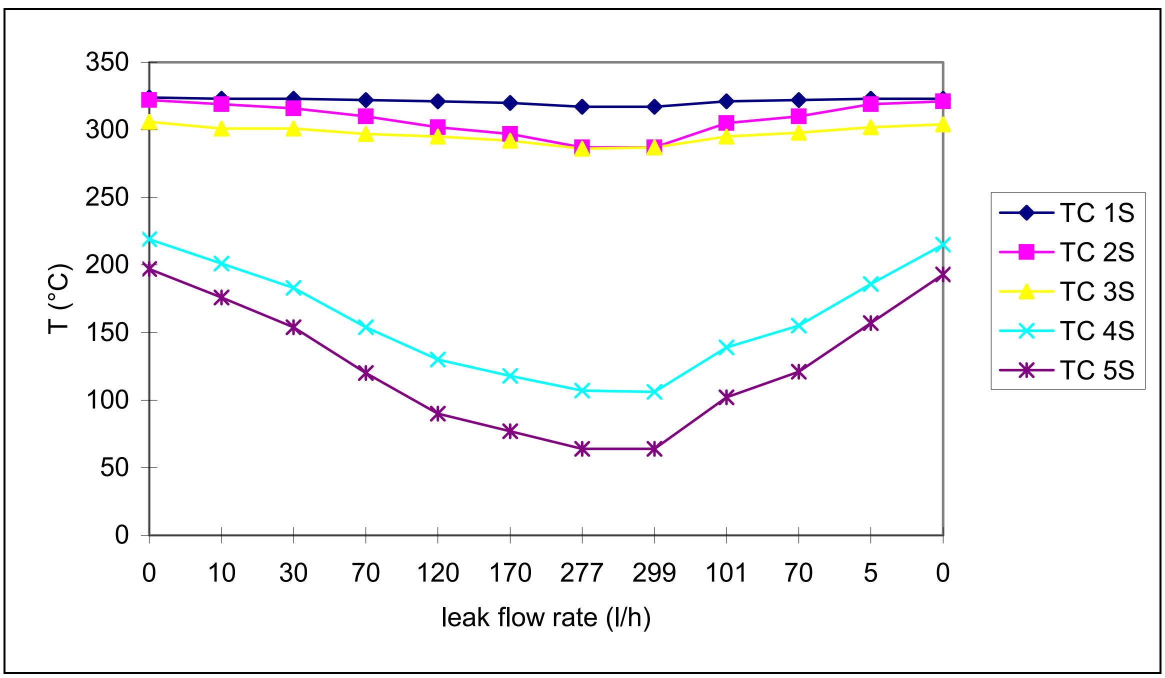

Figure C-5
Hot Leg 1 upper zone temperature evolution

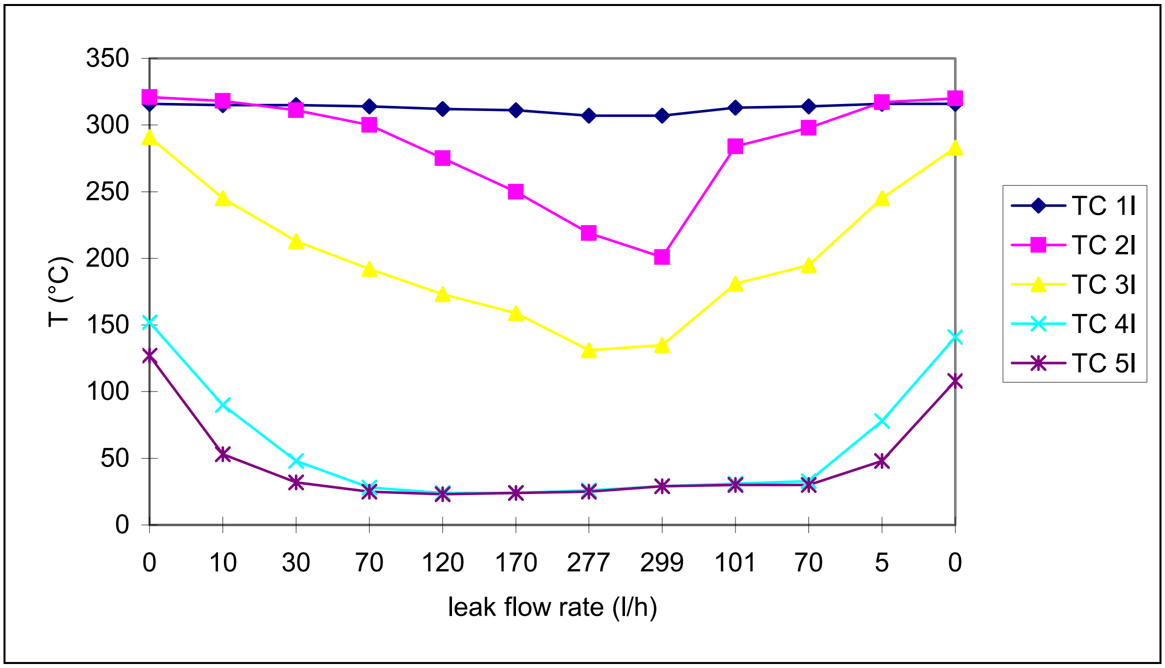

Figure C-6
Hot Leg 1 lower zone temperature evolution

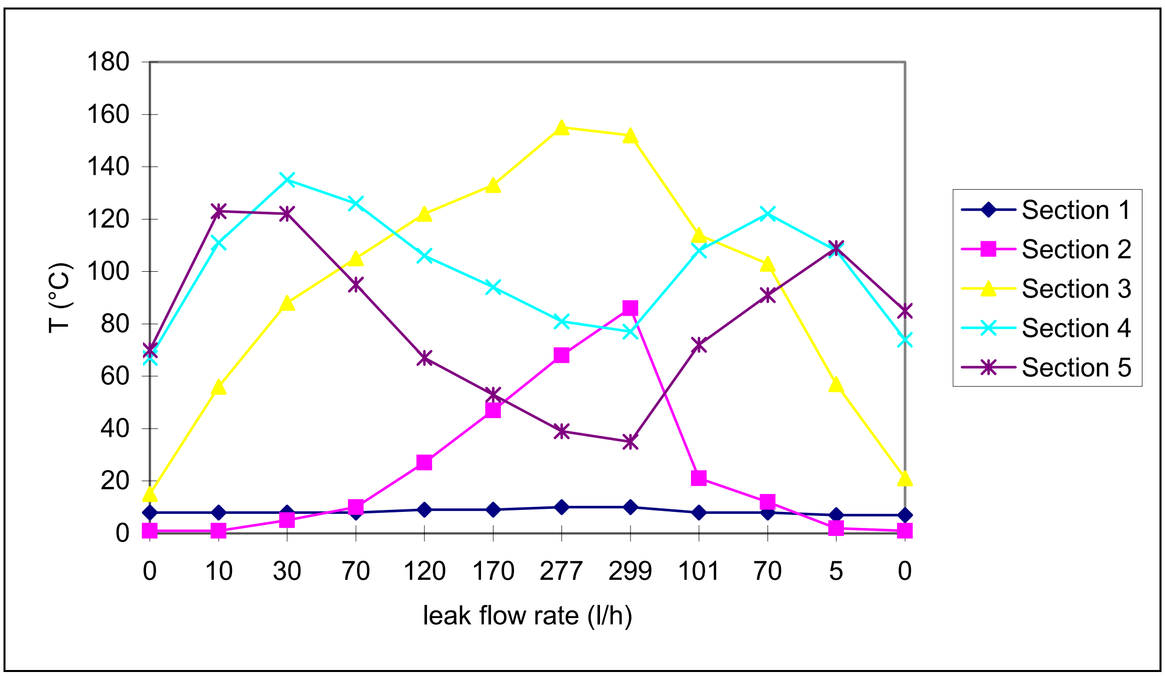

Figure C-7
Hot Leg 1 stratification evolution

Target:
Nuclear Power

About EPRI

EPRI creates science and technology solutions for the global energy and energy services industry. U.S. electric utilities established the Electric Power Research Institute in 1973 as a nonprofit research consortium for the benefit of utility members, their customers, and society. Now known simply as EPRI, the company provides a wide range of innovative products and services to more than 1000 energy-related organizations in 40 countries. EPRI's multidisciplinary team of scientists and engineers draws on a worldwide network of technical and business expertise to help solve today's toughest energy and environmental problems.

EPRI. Electrify the World

Printed on recycled paper in the United States of America

1003082

EPRI • 3412 Hillview Avenue, Palo Alto, California 94304 • PO Box 10412, Palo Alto, California 94303 • USA
800.313.3774 • 650.855.2121 • askepri@epri.com • www.epri.com